UNIVERSITA' DELL' INSUBRIA

FACOLTA' DI SCIENZE MATEMATICHE, FISICHE E NATURALI

Dottorato di Ricerca in Neurobiologia

Ph.D. Thesis

A novel role of CDKL5 in the regulation of mitotic spindle assembly and microtubule organization

Ph.D. Thesis of: Isabella Barbiero

Matr. N°: 701259

Supervisor: Prof. Charlotte Kilstrup-Nielsen

Assistant Supervisor: Prof. Nicoletta Landsberger

Coordinator: Prof. Daniela Parolaro

Cycle XXVIII 2012-2015

To the power of irrationality…

INDEX

ABSTRACT

Mutations in the *CDKL5* gene, located on Xp22, are the main cause of *CDKL5*-disorder characterized by the onset of epilepsy before 3 months of age, severe developmental delay and RTT-like features. Besides its functions in post-mitotic neurons, a recent work shows that the loss of CDKL5 influences the proliferation rate of neuronal precursors suggesting its role also in proliferating cells. However, the molecular mechanism through which CDKL5 acts on this cellular process is still unknown.

In this study we demonstrate the presence of CDKL5 at the mitotic centrosome and midbody. Importantly, the ablation of CDKL5 induces prolonged prometaphases, aberrant/multipolar spindle assembly and misaligned chromosomes. Furthermore, we show that, similar to many centrosomal proteins, CDKL5 influences microtubule organization. At the molecular level, we find that CDKL5 interacts with the scaffold protein IQGAP1, a regulator of Rac1, which regulates many cytoskeleton functions thanks to its ability to interact both with actin and plus end microtubule binding proteins (+TIPs). CDKL5 is required for the correct localization of IQGAP1 at the leading edge of polarized cells and down-regulation of CDKL5 reduces the capacity of IQGAP1 to interact with its effector proteins Rac1 and CLIP170, a +TIP that promotes microtubule stabilization at the cell cortex. Altogether, our data suggest that CDKL5 influences cell cycle progression through its centrosomal accumulation and cellular morphology through its interaction with microtubule associated proteins. We believe that these data will pave the way for a further understanding of the impact of CDKL5 in neuronal and non-neuronal cells.

1. INTRODUCTION

1.1 Rett syndrome: clinical features

Rett syndrome (RTT; OMIM 312750) is a severe X-linked neurodevelopmental disorder described for the first time in the 1960 by Andreas Rett (Rett, 1996) that affects approximately 1 in 10,000 female births. Typical RTT is caused by mutations in *Methyl-CpG-binding protein 2* (*MECP2)* and is characterized by *normal development* during the first 6-18 months of life followed by *developmental stagnation* (microcephaly, growth retardation, weight loss, and muscle hypotonia) and a *further decline* as the syndrome progresses (stereotypic movements, loss of language, ataxia, seizures, autonomic perturbations among other symptoms). The disease is also often accompanied by typical autistic traits such as lack of facial expression, hypersensitivity to sounds, lack of eye contact, indifference to social stimuli (Nomura, 2005). The last phase of the RTT is characterized by the appearance of parkinsonian-like symptoms (Hagberg, 2005; Roze et al, .2007), at this stage the pathological condition reaches a plateau and some patients can survive until the sixth or seventh decade of life in very serious and debilitating physical conditions (Chahrour et al., 2007). Beside classic RTT, several RTT variants with milder or more severe clinical pictures have been described and clustered into distinct clinical groups, such as *preserved speech variant*, *early seizure variant*, and *congenital variant* (Hagberg BA et al. 1994. Fig. 1).

About 95% of patients with classic RTT have mutations in *MECP2* (Williamson et al., 2006), but only 40-60% of individuals affected by RTT variants have mutations in this gene (Cheadle et al., 2000; Bourdon et al., 2001), suggesting the existence of other genes responsible of RTT.

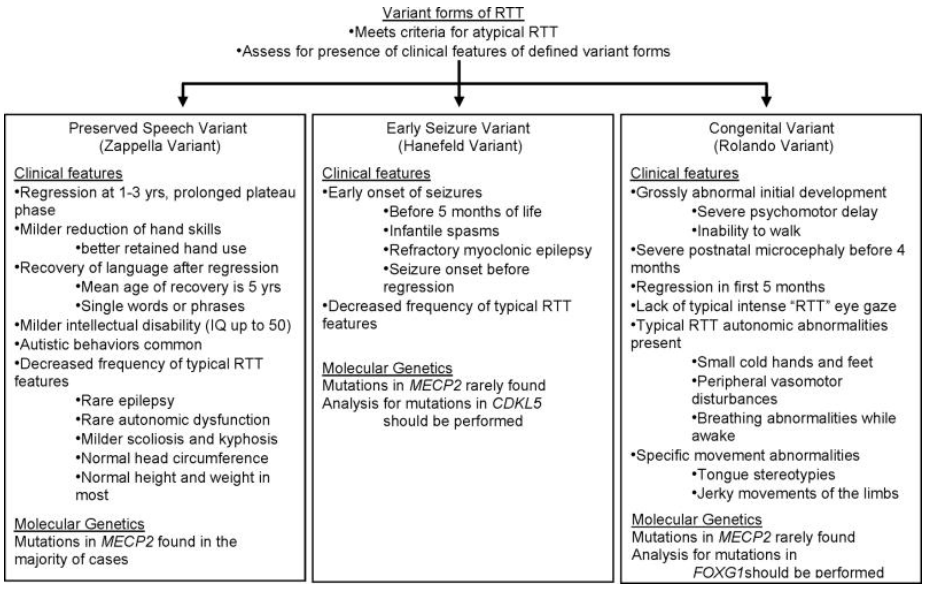

Figure 1 Variant forms of RTT (Neul et al, 2010)

1.2 CDKL5: from the discovery of the gene to the definition of the disease

CDKL5, first known as *STK9* (Serine Threonine Kinase 9) for its homologies with Serine Threonine Kinases, was identified for the first time in 1998 following a transcriptional mapping effort of the human chromosome Xp22, already known for genes associated with different diseases including Nance-Horan (NH) syndrome, oral-facial-digital syndrome type 1 (OFD1), and a novel locus for non-syndromic sensorineural deafness (DFN6) (Montini et al.,, 1998).

The link between *CDKL5* and human neuronal diseases was highlighted following the description of balanced translocations causing the destruction of the gene in two children suffering from West syndrome with serious intellectual disabilities and infantile spasms (Kalscheuer et al.,, 2003). Three years before, Hupopaniemi performed a mutation search in Danish patients and found a 136-kb deletion in two affected siblings with typical retinoschisis and epilepsy. The rearrangement partly deleted *XLRS1,* the gene implicated in X-linked juvenile retinoschisis (XLRS), and *PPEF-1* (protein phosphatase gene with EF calcium-binding domain) and truncated the 3' end of *STK9*, including the last coding exon. Since mutations in *XLRS1* had never been linked to seizures, the most plausible hypothesis was that epilepsy in these patients was caused by deletion of the CDKL5 C-terminal region (Huopaniemi et al.,, 2000). In 2004, Weaving and colleagues described two

different mutations of *CDKL5*, one familiar and one sporadic, in three patients with severe early-onset epilepsy with infantile spasms, mental retardation and clinical manifestation similar to RTT. *CDKL5* was thus proposed as a novel gene implicated in the "early seizure variant" of Rett syndrome (Weaving et al., 2004), also known as the Hanefeld variant in honour of the Swedish doctor who described it in 1985 for the first time (Hanefeld, 1985). Ever since, other clinical phenotypes have been described in patients mutated in *CDKL5* using different terminology as: "ISSX and mental retardation" (Kalscheuer et al., 2003), "Atypical RTT", "Early-onset seizure variant of RTT", "Autistic disorder with intellectual disability", "Profound intellectual disability and seizures" (Weaving et al., 2004), "Neonatal onset encephalopathy", "Severe neurodevelopmental retardation" (Tao et al., 2004), "Rett syndrome variant with infantile spasms" (Scala et al., 2005), "Severe infantile encephalopathy" (Rosas-Vergas et al., 2007), "Severe encephalopathy and early-onset intractable epilepsy" (Elia et al., 2008). In order to simplify the terminology, these phenotypes have been gathered together under the name of "*CDKL5*-related disorders" or "*CDKL5*-associated encephalopathy" (Bahi-Buisson et al., 2008a).

A full understanding of the clinical picture of *CDKL5*-related disorders is still limited and a larger series of patients is required to further understand its presentation and natural history. In this regard, Bahi-Buisson and colleagues tried to define the clinical profile of *CDKL5*-associated encephalopathy, screening the whole coding region of *CDKL5* in a total of 183 patients with early encephalopathy; 20 patients with pathogenic *CDKL5* mutations including 7 novel sequence variations were described together with the clinical features of patients published so far. In particular, in younger patients before 2 years of age, early onset epilepsy appears as the most consistent sign of *CDKL5* mutations. In all cases, epilepsy starts within 3 months with very frequent seizures and an interictal EEG pattern that is normal or shows a slowing background. At this age, neurological examination reveals severe hypotonia and poor eye contact, but none of the RTT-like features observed in later ages. More rarely, after a minimum of milestones have been acquired, a phase of regression can follow with decelerated growth of the head circumference, while, starting from the second/third year of life and not in all patients, some RTT-like features could appear such as stereotypic movements, apraxia and sleep disorders. Finally, the patients with *CDKL5*

mutations described in Bahi-Buisson's study, never demonstrated the characteristic EEG development observed in typical RTT (Hagne et al., 1989). Seizures may be of various natures and may occur in the same patient depending on the progression of the disease. In this regard, Bahi-Buisson suggests a trend characterized by three phases: an early phase (1-10 weeks old) with frequent generalized tonic seizures, a second phase (from 6 months to 3 years old) with spasms and epileptic encephalopathy and a later stage dominated by the persistence of tonic seizures and by the appearance of myoclonic seizures (Bahi-Buisson et al., 2008b).

Summarizing, according to Bahi-Buisson the key clinical features of CDKL5 disorder are early epilepsy with very frequent seizures, severe hypotonia, poor eye contact and some RTT-like features, such as secondary deceleration of head growth, severe motor impairment, sleep disturbances, hand apraxia and hand stereotypies (Fig. 2).

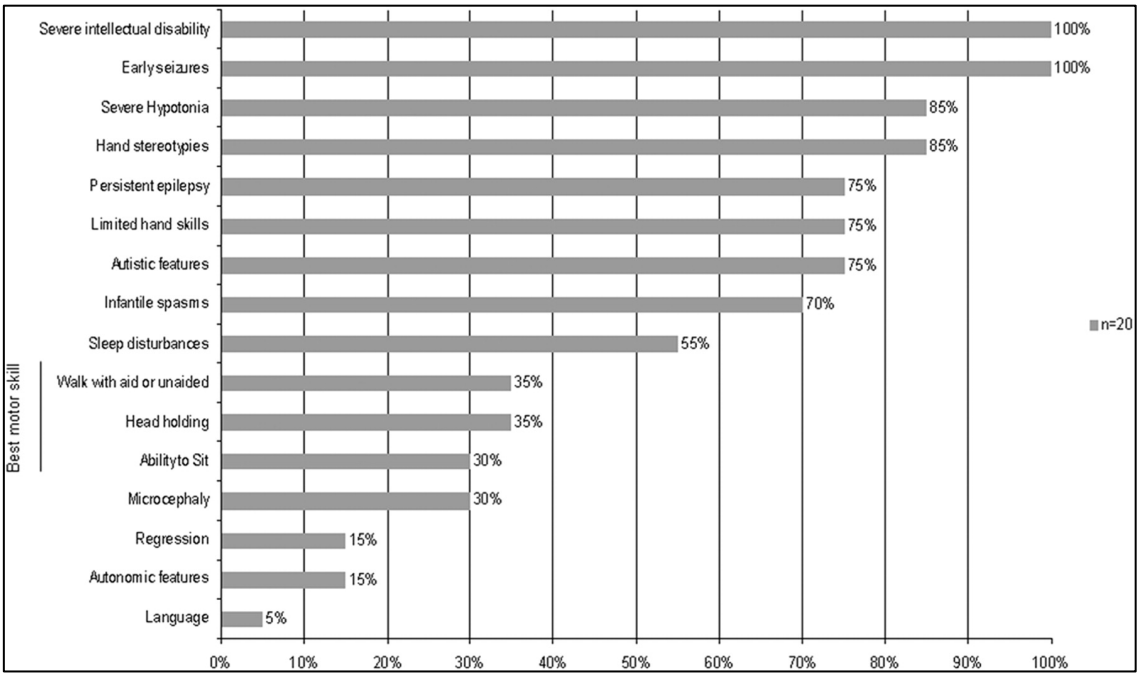

Figure 2 Prevalence of 18 clinical features in 20 CDKL5 mutation patients (Bahi-Buisson et al., 2008a)

After Bahi-Buisson, in 2010 Artuso tried once again to delineate the specific clinical diagnostic criteria for *CDKL5* disorder, reporting the investigation of 9 girls with *CDKL5* mutations plus clinical features of other 34 patients already described in literature. According to the previous work, early epilepsy with an onset between

the first week and 5 months was defined as the main criteria for the identification of *CDKL5* mutations (Fig. 3). In addition, the presence of stereotypic hand movements typical of RTT, such as hand mouthing, washing or clasping, severe hypotonia and impaired psychomotor development were considered other hallmarks of the disease. According to Artuso et al., *CDKL5* patients presented a normal prenatal history and a quite normal perinatal period, poor eye contact and absence of response to social interactions, absence of speech, absence of hand skills and neurovegetative dysfunctions such as gastrointestinal disturbances and breathing irregularities (Artuso et al., 2010).

Necessary criteria
- Normal prenatal history
- Irritability, drowsiness and poor sucking in the perinatal period before the seizures onset
- Early epilepsy, with an onset between the first week and 5 months
- Hand stereotypies
- Severely impaired psychomotor development
- Severe hypotonia

Supportive criteria
- Infantile spasm at onset or during the course of epilepsy
- Poor eye contact and absence of response to social interactions
- Absence of speech
- Absence of hand skills
- Absence of scoliosis
- Normal head circumference at birth that remains normal or has a slight deceleration of growth
- Normal weight and height
- Rare neurovegetative dysfunctions: gastrointestinal disturbances, breathing irregularities, cold extremities

Figure 3 Diagnostic criteria for early-onset seizure variant of RTT (Artuso et al., 2010)

The criteria followed by Bahi-Busson and Artuso to classify *CDKL5*-associated encephalopathy as atypical RTT variant were those defined by Hagberg in 1995 (Hagberg BA et al., 1994), but the increasing number of patients mutated in CDKL5 and the expanded knowledge of RTT, necessitated to reconsider the diagnostic criteria for RTT and its variants. In 2010, Neul and colleagues in collaboration with the Rett Search Consortium, revised and simplified the diagnostic criteria for typical and atypical RTT. They identified three groups of criteria: *main* criteria, *exclusion* criteria and *supportive* criteria (Fig. 4) and limited the necessary criteria for both classic and variant RTT to the presence of regression (loss of purposeful hand use and spoken language, development of gait abnormalities and hand stereotypies) and added other four main criteria that are absolutely required for

the diagnosis of typical RTT (listed as main criteria in the table in figure 4). For a diagnosis of atypical RTT, besides the presence of regression, Neul et al. suggested that 2 out of the 4 main criteria and 5 out of 11 supportive criteria should be present.

However, an interesting work of Fehr and colleagues was published in 2013, in which the phenotype of 77 females (from 6 months to 22.4 years) and 9 males (from 1.1 to 14.9 years) with a pathogenic or potentially pathogenic CDKL5 mutation, identified through the International Rett Syndrome Phenotype Database (InterRett), was compared to Neul's criteria for early seizure variant of RTT (ESV) (Fehr et al., 2013). Overall, only 23.7% of females and no males fulfilled all criteria for ESV RTT described above. This was largely due to the absence of regression in all males and in 67.5% of females, in accordance with the precedent studies of Bahi-Buisson and Artuso (Bhai-Buisson et al., 2008a; Artuso et al., 2010). Several of the specific supportive criteria, such as diminished response to pain, a spinal curvature and intense eye pointing, were also infrequently reported. Some of these supportive characteristics appear age-dependent and were observed more commonly in patients aged over 5 years. Interestingly, dysmorphic features were identified that could be useful for the diagnosis of CDKL5 disorder. Indeed, CDKL5 patients are frequently characterized by prominent and/or broad forehead, high hairline, relative midface hypoplasia, deep-set but large appearing eyes and infra-orbital shadowing (Fig.5) (Fehr et al., 2013). In conclusion the author proposes, for the first time, to consider CDKL5 disorder as separated to RTT, rather than a RTT variant and suggests that the clinical picture of females and males with the CDKL5 disorder should not only concentrate on features that should be present in RTT, but also on the features that are present in the CDKL5 disorder.

Even if it seems that boys with CDKL5 disorder tend to be more severely affected than females, it is still difficult to make a precise comparison between both sexes (Fehr et al., 2015). Surely, X-inactivation resulting in a mosaic expression of normal and mutant CDKL5 protein in female patients may result in a more positive outcome, but it is also true that a huge hetereogenity between male patients exists; further studies will be necessary to clarify this point.

Necessary criteria						
A period of regression followed by recovery or stabilisation	10/41 (24.4)	15/36 (41.7)	25/77 (32.5)	1/6 (16.7)	0/3 (0.0)	1/9 (11.1)
Main criteria						
Partial or complete loss of acquired purposeful hand function	4/36 (11.1)	7/30 (23.3)	11/66 (16.7)	0/5 (0.0)	0/3 (0.0)	0/8 (0.0)
Partial or complete loss of acquired spoken language	8/40 (20.0)	6/35 (17.1)	14/75 (18.7)	0/6 (0.0)	0/3 (0.0)	0/9 (0.0)
Gait abnormalities: Impaired (dyspraxic) or absence of ability	40/40 (100.0)	27/34 (79.4)	67/74 (90.5)	6/6 (100.0)	3/3 (100.0)	9/9 (100.0)
Stereotypic hand movements	32/41 (78.0)	29/35 (82.9)	61/76 (80.3)	3/6 (50.0)	0/3 (0.0)	3/9 (33.3)
Supportive criteria						
Breathing disturbances when awake	19/38 (50.0)	17/33 (51.5)	36/71 (50.7)	3/6 (50.0)	2/3 (66.7)	5/9 (55.5)
Bruxism when awake	33/40 (82.5)	30/33 (90.9)	63/73 (86.3)	5/5 (100.0)	3/3 (100.0)	8/8 (100.0)
Impaired sleep pattern	31/36 (86.1)	31/33 (93.9)	62/69 (89.8)	5/5 (100.0)	2/3 (66.7)	7/8 (87.5)
Abnormal muscle tone	13/15 (86.7)	10/11 (90.0)	23/26 (88.5)	2/2 (100.00)	NA	2/2 (100.0)
Peripheral vasomotor disturbances	11/40 (27.5)	19/33 (57.6)	30/73 (41.1)	1/5 (20.0)	2/3 (66.7)	3/8 (37.5)
Scoliosis/kyphosis	1/39 (2.6)	14/34 (41.2)	15/73 (20.5)	0/5 (0.0)	3/3 (100.0)	3/8 (37.5)
Growth retardation	6/10 (60.0)	6/9 (66.7)	12/19 (63.1)	0/2 (0.0)	Missing	0/2 (0.0)
Small cold hands or feet	19/39 (48.7)	24/31 (77.4)	43/70 (61.4)	2/5 (40.0)	2/3 (66.7)	4/8 (50.0)
Inappropriate laughing/screaming spells	22/35 (62.9)	29/32 (90.6)	51/67 (76.1)	3/5 (50.0)	1/3 (33.3)	4/8 (50.0)
Diminished response to pain	15/37 (40.5)	11/31 (35.5)	26/68 (38.2)	0/5 (0.0)	1/3 (33.3)	1/8 (12.5)
Intense eye communication 'eye pointing'	5/37 (13.5)	5/33 (15.1)	10/70 (14.3)	0/5 (0.0)	0/3 (0.0)	0/8 (0.0)
ESV-specific criteria						
Early-onset seizures before 5 months of age	40/40 (100.0)	32/35 (91.4)	72/75 (96.0)	6/6 (100.0)	3/3 (100.0)	9/9 (100.0)
Infantile spasms[a]	11/22 (50.0)	3/14 (21.4)	14/36 (38.9)	1/3 (33.3)	1/1 (100.0)	2/4 (50.0)
Refractory myoclonic epilepsy[b]			NA			
Seizure onset before regression	40/41 (97.6)	30/36 (83.3)	70/77 (90.9)	4/5 (80.0)	3/3 (100.0)	7/8 (87.5)
Decreased frequency of typical RTT features[c]			NA			
Meets criteria for atypical RTT						
Necessary criteria	10/41 (24.4)	15/36 (41.7)	25/77 (32.5)	1/6 (16.7)	0/3 (0.0)	1/9 (11.1)
Two of the four main criteria	32/40 (80.0)	25/33 (75.8)	57/73 (79.5)	3/6 (50.0)	0/3 (0.0)	3/9 (33.3)
5 Of the 11 supportive criteria	20/28 (71.4)	26/26 (100.0)	46/54 (86.4)	2/3 (66.7)	3/3 (100.0)	5/6 (83.3)
All criteria	7/39 (17.9)	12/36 (33.3)	19/75 (23.7)	0/6 (0.0)	0/3 (0.0)	0/9 (0.0)

Figure 4 Proportion of females (n = 77) and males (n = 9) that met each of the latest criteria for ESV RTT defined by Neul in 2010 (Fehr et al., 2013)

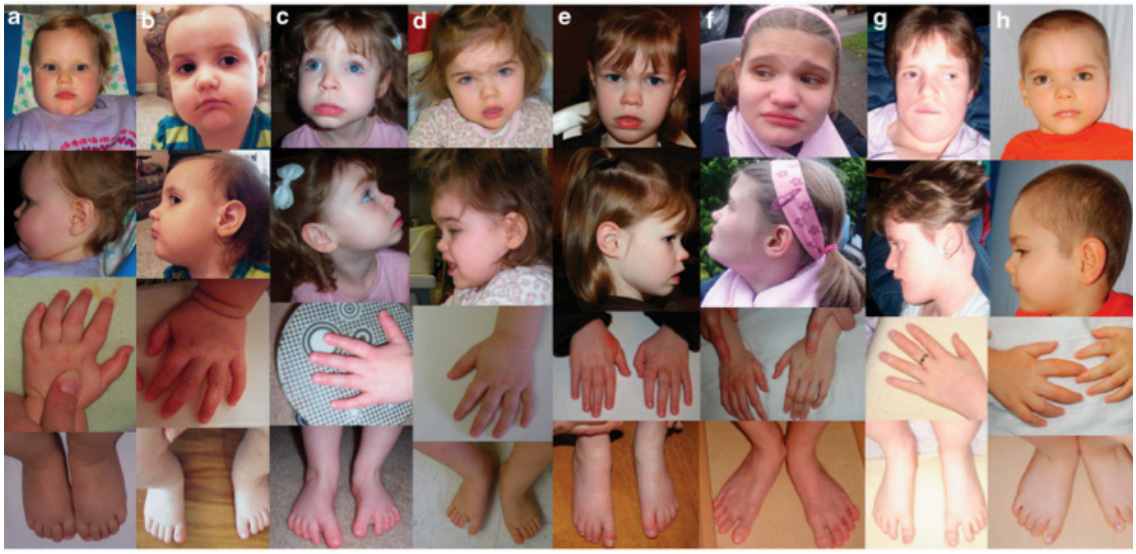

Figure 5 "Examples of identified facial, hand and feet features in males and females with the CDKL5 disorder (n=67)" (Fehr et al., 2013)

1.3 CDKL5 gene and isoform

CDKL5 is composed by 24 exons; the first three exons (exons 1, 1a, 1b) are transcribed but not translated and the ATG start codon is located within exon 2.

Alternative splicing results in the formation of at least three protein isoforms that differ in the C-terminal domain. The first isoform generates a protein of 1030 amino acids with a molecular weight of 115 kDa that is expressed primarily in the testes (Fig. 6). The second isoform of 960 amino acids (107 kDa) was identified later and is the prevailing brain isoform. $CDKL5_{115}$ contains exons 19-21 that are not retained in $CDKL5_{107}$. A brain specific exon, 16b, has been discovered in human and mouse *CDKL5/Cdkl5* mRNAs but whether it is included in $CDKL5_{115}$ and/or $CDKL5_{107}$ still needs to be determined (Williamson et al., 2012).

Interestingly, a shorter CDKL5 isoform has been identified specifically in rat glial cells. The glial isoform may be relevant for glial development since its expression is induced during the perinatal/postnatal stages when a rapid onset of massive gliogenesis starts (Chen et al., 2010).

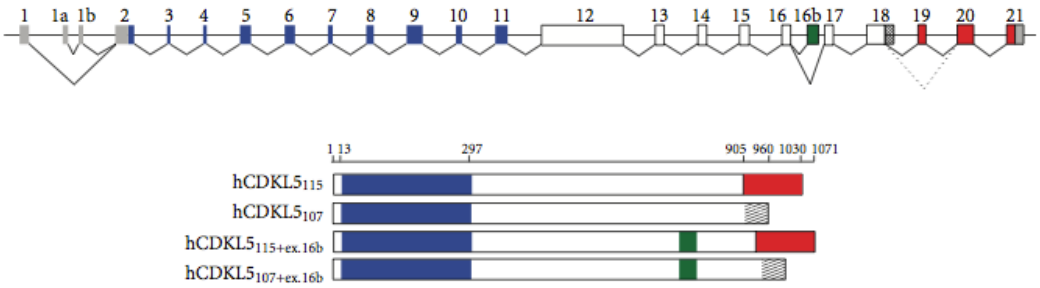

Figure 6 Schematic representation of human *CDKL5* gene (top) and its variants generated by alternative splicing (button). In grey are indicated the non-translated sequences, in blue the sequences coding for the catalytic region, in white the exons present in all isoforms, and in green, red and dashed the isoform - specific exons (adapted by Williamson et al., 2012).

1.4 CDKL5 protein

CDKL5 is a serine/threonine kinase that shares homology with members of the mitogen-activated protein (MAP) kinase and cyclin-dependent protein kinase-like (CDKL) families (Montini et al., 1998). CDKL5 is characterized by a catalytic domain (aa 13-297) at the N-terminus and a long C-terminal tail; the catalytic domain comprises an ATP-binding region (amino acids 14–47) and a serine-threonine protein kinase active site (amino acids 127–144) whereas in the C-terminal domain two putative nuclear import (NLS) and export signals (NES) are localized. CDKL5 contains within its catalytic domain a so called TEY (Thr-Glu-Tyr) (aa 169-167) motif whose dual phosphorylation is normally involved in activating

kinases of the MAP-kinase family (Herbert et al., 2002). Interestingly, the autocatalytic activity of CDKL5 allows it to auto-phosphorylate directly this motif (Bertani et al., 2006).

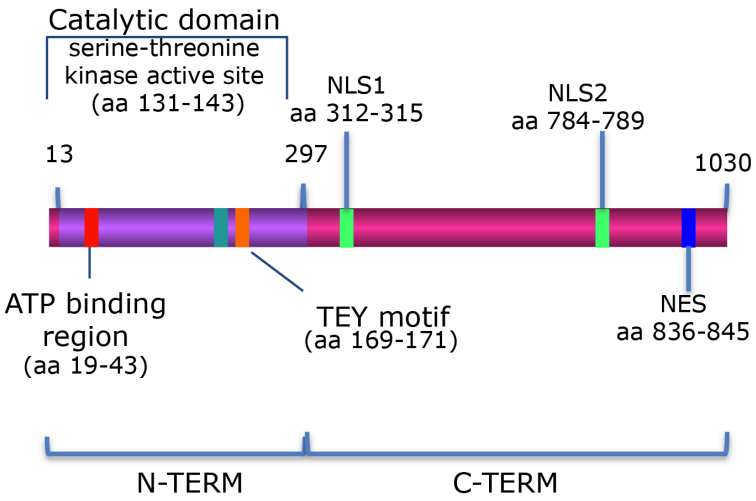

Figure 7 Schematic representation of CDKL5$_{115}$. NLS (nuclear import signal), NES (nuclear export signal).

Of great importance for the cellular localization of CDKL5 is the carboxy-terminal tail. In fact, mutations in this site seem to interfere with the proper localization of the protein. In particular, contrary to the wild-type protein, the truncated pathologic CDKL5 mutants R781X and L879X remain confined almost exclusively in the nucleus (Bertani et al, 2006; Rusconi et al, 2008). The cytoplasmic localization of the wild-type protein depends on the nuclear export receptor CRM1. However, the NES-like sequence in the C-terminal tail (aa 863-865), which is present in the L879X derivative, seems insufficient for the exit of the mutant protein from the nucleus to the cytoplasm, suggesting that other signals are involved in regulating the subcellular localization of CDKL5.

A precise consensus for target recognition by CDKL5 is not yet clear but recently works, based on mutagenesis studies with the CDKL5 substrate Amph1, which plays a key role in clathrin-mediated endocytosis of synaptic vesicles (Katayama et al., 2015; Sekiguchi et al., 2013), suggested RPXSX as putative consensus sequence. Although this study might represent a preliminary starting point to identify other targets of CDKL5, the lack of the same sequence in other CDKL5 substrates described in literature, calls for further studies to better understand the molecular basis that governs the relationship between this kinase and its interactors.

1.5 CDKL5 pathological mutations

The phenotypes associated with *CDKL5* mutations range from a milder form, where the epilepsy is controlled and independent ambulation is achieved, to a severe form with microcephaly, no motor development and refractory epilepsy. The severity of the disease is influenced by genetic and epigenetic factors. For sure the clinical picture of CDKL5 patients depends on the proportion of functional and dysfunctional CDKL5 produced by the normal or mutated alleles due to X-chromosome inactivation (XCI). Random XCI leads to equal inactivation of the maternal or the paternal X chromosome whereas the inactivation is "skewed", when the same X is silenced in the majority of cells (J. Brown, 1998).

CDKL5 mutations can be of various types: missense, nonsense, splice site mutations, deletions, insertions, translocations and large genetic rearrangements. Generally, all these mutations occur de novo. Analysing the distribution of missense mutations, it appears that these involve almost exclusively the catalytic domain, whereas truncating mutations may occur along the entire protein. In this regard, thanks to the experiments carried out in our laboratory, it was possible to demonstrate how point mutations in the kinase domain can greatly reduce the catalytic activity of the kinase. Conversely, truncating mutations in the downstream C-terminus cause an increased catalytic activity and the nuclear accumulation of CDKL5, suggesting the importance of the C-terminal tail in controlling the activity and localization of the kinase (Bertani et al., 2006; Rusconi et al., 2008). According to Bahi-Buisson, truncating or missense mutations in the catalytic domain should cause a more severe clinical phenotype characterized by higher incidence and more precocious onset epileptic encephalopathy than that caused by truncating mutations located in the last exons of *CDKL5* (Bahi-Buisson et al., 2008b). This assumption, however, has been challenged by another group, noting that to date it is still premature to predict a genotype-phenotype correlation, given the limited number of patients (Fehr et al., 2015).

Recently, Szafranski and his collaborators report seven females and four males from seven unrelated families with genomic duplications including *CDKL5*. Interestingly, whereas 55% of patients with *CDKL5* genomic deletions or point mutations have acquired progressive microcephaly, 3 out of the 11 patients had

macrocephaly. Moreover, unlike CDKL5 deficiency, none of the duplicated patients had epilepsy. Further, the patients were characterized by difficulties in learning, autistic and hyperactive behaviour, developmental and speech delay. In conclusion, not only loss but also gain-of-function of CDKL5 causes neurological phenotypes, underlining for the first time the importance of CDKL5 dosage effects. Increased dosage of CDKL5 was proposed to affect the global output of the interactions of CDKL5 with its substrates, leading to perturbation of synaptic plasticity and development (Szafranski et al., 2015). Of relevance, these findings have also severe implications for the development of gene therapy approaches against CDKL5-disorder.

1.6 Regulation of CDKL5 expression and subcellular localization

Proteins are synthesized and regulated depending upon the functional need of the single cell. The knowledge of a given protein's expression pattern is therefore instrumental to understand its roles within an organism. *Cdkl5* mRNA has been identified in brain but also in peripheral tissues, thus suggesting its involvement in both terminally differentiated and in dividing cells (Williamson et al., 2012).
In brain, *Cdkl5* mRNA is expressed at higher levels in some cortical areas (frontal cortex, motor cortex and cingulate gyrus, entorhinal cortex), responsible for "higher-order" functions like language and information processing, and in all three CA fields of the hippocampus, important for learning and memory. Very high levels of *Cdkl5* transcripts are also detected in thalamic nuclei, involved in sensory and motor signal relay and in the regulation of consciousness and sleep, while lower transcript levels are detected in the cerebellum, implicated in coordination of motor movements. Considering different neuronal subtypes, *Cdkl5* mRNA is predominantly expressed in glutamatergic and gabaergic neurons and at very low levels in dopaminergic areas such as the substantia nigra or the ventral tegmental area or in noradrenergic areas such as the locus coeruleus (Kilstrup-Nielsen et al., 2012).

In periphery, *Cdkl5* mRNA can be detected in testis, lung, spleen, placenta, uterus, prostate and thyroid (Williamson et al, 2012).

Western blot analyses of CDKL5 protein expression in mice and rats confirm the trend of the transcript profile (Rusconi et al, 2008; Chen et al., 2010). Interestingly, CDKL5 is lowly expressed during embryogenesis but is strongly induced during the postnatal period, reaching its highest expression at postnatal day 14 (P14), where after it slowly begins to decline (Rusconi et al., 2008). These data correlate with the importance of CDKL5 in the process of neuronal maturation. At the subcellular level, CDKL5 is, as previously described, shuttling between the cytoplasm and the nucleus where it seems to be implicated in the regulation of alternative splicing (Ricciardi et al., 2009) and in the regulation of gene expression through its interaction with MeCP2 (Mari et al., 2005) and DNMT1 (Kameshita et al., 2008).

Interestingly, the neuronal localization of CDKL5 is mainly cytoplasmic during embryogenesis whilst the nuclear fraction increases during the early postnatal stages, concurrent with neuronal maturation, and remains abundant until adulthood (Rusconi et al., 2008).

1.7 Role of CDKL5 in post-mitotic neurons and in proliferating cells: what are the consequences of its ablation?

1.7.1 Role of CDKL5 in post-mitotic neurons

For convenience we can reassume defects due to the absence of CDKL5 into three groups: behavioural, morphological and molecular defects.

- *Behavioural defects*

To date, the use of animal models is necessary to understand the molecular mechanisms underlying the onset of a disease and, although they cannot summarize all aspects of a disorder, they are generally regarded as an excellent tool to study the functions of a specific protein. Thanks to the development of

Cdkl5 knockout (KO) mouse models it has been possible to confirm and complement the information previously obtained with the technique of RNA interference with those produced *in vivo*. Although it is not always possible to compare the interference and the knockdown system, similarities have been observed between the two models.

The first *Cdkl5* knockout mouse (C57BL/6 background) was published three years ago by the group of Zhaolan Zhou (Wang et al., 2012); it was generated by the deletion of *Cdkl5* exon 6 through homologous recombination in ES cells, causing an early truncation of CDKL5 in the N-terminal kinase domain. *Cdkl5*$^{-/y}$ mice present hyperactivity, impaired motor control (hindlimb and forelimb clasping) and decreased anxiety similar to those observed in RTT and autism spectrum disorder (ASD) mouse models (Chahrour et al., 2007; Schmeisser et al., 2012). Interestingly, mice lacking CDKL5 demonstrate profound impairment in social interaction and deficient contextual and cued fear memory. Brain size is comparable with that of wild-type littermates and even if intractable seizures are a hallmark of CDKL5 disorder, video-EEG monitoring did not reveal spontaneous seizures in *Cdkl5*$^{-/y}$ mice. However, recording of event-related potential (ERP), which is an electrophysiological response of cognitive processes, showed attenuated and delayed ERP polarity peaks suggesting impaired neuronal connectivity (Wang et al., 2012).

One year ago, Amendola et al. published another mouse model (C57BL/6J background) carrying a targeted conditional knockout allele of *Cdkl5* that was generated through the deletion of *Cdkl5* exon 4 (Amendola et al., 2014). According to the previous work, these *Cdkl5*$^{-/y}$ mice did not reveal either spontaneous epileptiform activity or abnormal brain size; moreover, clasping of hindlimbs denote motor impairment. In contrast to the first model, Amendola's mouse model showed a significant decrease in locomotion in both homozygous females and hemizygous males in a home cage activity test. The difference could depend on the type of test and how the behaviour was measured; indeed, in the first case, locomotor activity was measured by beam breaks in a photobeam frame (Med Associates) and was quantified over 60 min in 5-min bins (Wang et al., 2012). In the second case, activity was monitored continuously for four days and binned into 12 h epochs (Amendola et al., 2014).

Altogether, the *Cdkl5* KO mouse models recapitulate many core features of CDKL5 disorders and appear to be an important support to understand the molecular mechanisms underlying the pathology in order to identify therapies targeted at slowing down or reversing disease progression.

- *Morphological defects*

At the morphological level, *Cdkl5*$^{-/y}$ cortical and hippocampal pyramidal neurons show reduced dendritic arborization with a significant reduction in cortical thickness (Amendola et al., 2014; Fuchs et al., 2014), underscoring the function of CDKL5 for correct neuronal development and confirming the previous data obtained *in vitro* by Chen et al. (Chen et al., 2010). This aspect was also observed by Ricciardi et al., who investigated the role of CDKL5 in dendritic spines (Ricciardi et al., 2012). They demonstrated that CDKL5 is almost exclusively localized at excitatory synapses both *in vitro* and *in vivo*. Importantly, they observed that hippocampal neurons silenced for CDKL5 showed a significant increase in protrusion density and that the protrusions had a filopodia-like morphology characteristic of an immature stadium of spine development. The morphological alterations reported in *Cdkl5*-silenced neurons were associated with a reduction in the number of excitatory synapses and synaptophysin puncta *in vitro* and *in vivo* and also in iPSC lines from two female patients diagnosed with CDKL5 pathogenic mutations (R59X, L220P) (Ricciardi et al., 2012).
The morphological defects caused by the lack of CDKL5 suggest its implication in the regulation of cytoskeleton, a hypothesis that seems to be confirmed by the fact that CDKL5 interacts with ***Rac1***, a Rho GTPase involved in the remodelling of actin and microtubule cytoskeleton (Wittmann et al., 2001); furthermore, this interaction is favoured by brain-derived neurotrophic factor (BDNF) (Chen et al., 2010). It is worth mentioning that mutations in members of the Rho GTPase family have been identified in patients characterized by mental retardation (Remakers, 2002). The involvement of CDKL5 in mechanisms that govern cytoskeleton remodelling is consistent with the results published by Ricciardi and colleagues showing that loss of CDKL5 in rat neurons elicits an increased number of filopodia-like spines and reduced synaptic strength (Riacciardi et al., 2012). In the same

work, they demonstrated that CDKL5 interacts with ***NGL***s, which are synaptic cell adhesion molecules (CAMs) that exert a role in synapse homeostasis. Importantly, CDKL5 was found capable of phosphorylating NGL-1 at Ser 631 both *in vitro* and in mouse brain and this phosphorylation event appears to mediate NGL1-binding to PSD95 at the excitatory synapses.

Altogether, the capacity of CDKL5 to regulate neuronal morphogenesis likely through cytoskeleton remodelling via BDNF-Rac1 signalling and NGL-1-PSD95 interaction provides new mechanistic insights into how CDKL5 mutations might impact neuronal functions in CDKL5-related neurodevelopmental disorders. Another cytoplasmic substrate of CDKL5 is, as already mentioned, ***amphiphysin 1*** (AMPH1), which is a multifunctional adaptor molecule involved in neurotransmission and synaptic vesicle recycling through clathrin-mediated endocytosis (Sekiguchi et al., 2013). Amph1 is known to be involved in the interaction with endophilin, and phosphorylation of Ser/Thr residues in the PRD region of Amph1 reduced its affinity for endophilin (Murakami et al., 2006). In the present study, the authors demonstrated that CDKL5 phosphorylates Amph1 on Ser 293 and by pull-down experiments with phospho-mimetic and phospho-defective mutants they demonstrated that Ser 293 phosphorylation negatively influences Amph1 binding to endophilin. It is worth noting that Rac1 is able to influence the internalization of its specific targets by clathrin-mediated endocytosis (Cobbold et al., 2003); this is another aspect that underlies once again the importance of CDKL5 in neuronal morphogenesis through cytoskeleton rearrangements.

- *Molecular defects*

Since CDKL5 is a protein kinase, the analysis of how phosphorylation profiles are altered by its absence is highly relevant to understand the molecular pathways influenced by CDKL5 and representing possible therapeutic targets. This was addressed by Wang et al. using *Cdkl5*$^{-/y}$ mice. A Serine/Threonine (S/T) kinome profiling was performed in striatum, cortex, hippocampus and brainstem using antibodies developed against a large set of well-characterized S/T phosphorylation motifs. With this approach strongly, moderately or mildly affected

phosphorylation profiles were observed. Among the strongly affected signalling cascades was that of AKT–mTOR. Indeed, reduced phosphorylation was detected of rpS6, a ribosomal regulatory subunit and modulator of protein translation whose activation is regulated by AKT (Wang et al., 2012). Accordingly, reduced phosphorylation of rpS6 and AKT was also observed in Amendola's mouse model confirming the inhibition of this pathway (Amendola et al., 2014). This is of particular interest because mutations and dysfunction of components of this pathway have been linked to ASDs, RTT, and epileptic encephalopathies (Chen et al., 2014; Ricciardi et al., 2011).

1.7.2 Role of CDKL5 in proliferating cells

The association of CDKL5 with neurological diseases has pushed forward the studies of its functions in the central nervous system. However, its ubiquitous expression and the significant homology with members of the MAP and cyclin-dependent kinases, which are well known regulators of cell cycle progression, leads to hypothesize a role of CDKL5 also in proliferating cells. In this regard, a recent study of Fuchs et al. described a new function of CDKL5 in the process of adult neurogenesis (Fuchs et al., 2014).

Active adult neurogenesis is spatially restricted under normal conditions to two specific "neurogenic" brain regions: the subgranular zone (SGZ) in the dentate gyrus of the hippocampus where new dentate granule cells are generated, and the subventricular zone (SVZ) of the lateral ventricles where new neurons are generated and then migrate through the rostral migratory stream (RMS) to the olfactory bulb to become interneurons (Gage, 2000). In the SGZ, proliferating radial and non-radial precursors give rise to intermediate progenitors, which in turn generate neuroblasts that will be committed to the neuronal fate. Immature neurons migrate into the inner granule cell layer and differentiate into dentate granule cells in the hippocampus. Within days, newborn neurons extend dendrites toward the molecular layer and project axons through the hilus toward the CA3 (Zhao et al., 2006).

A quantitative analysis revealed that the number of BrdU positive progenitor cells (NPCs) in the dentate gyrus (DG) at P45 was higher in both *Cdkl5*$^{-/-}$ and *Cdkl5*$^{-/Y}$

mice compared to wild type animals suggesting that CDKL5 exerts a negative role on cell proliferation (Fuchs et al., 2014). However, the same experiment performed one month later (P75) revealed no difference in the number of BrdU labelled cells, indicating that the surplus of cells born at P45 was bypassed by a reduction in survival rate. Accordingly, an increase of active apoptotic cell death was observed in early post-mitotic neurons. Interestingly, the number of astrocytes did not change, demonstrating that the loss of Cdkl5 specifically affects survival of post-mitotic neurons without affecting astrogliogenesis (Fuchs et al., 2014).

These data indicate that CDKL5 influences the balance between mitotic cells and differentiating neurons in an opposite manner. In accordance with previous publications, the morphological analysis of neurite outgrowth in α-tubulin III positive cells revealed that neurons generated from *Cdkl5*$^{-/-}$ NPCs were less differentiated in comparison with wild type neurons (Chen et al., 2010; Amendola et al., 2014). Moreover, the present study confirmed the deranged AKT signalling *in vivo* and in differentiated NPCs. In particular, when the activity of the AKT/GSK-3β pathways was compared in *Cdkl5* KO and WT mice, lower phosphorylation levels were observed of PDK1 (3-phosphoinositide-dependent protein kinase 1, which activates AKT), AKT (at residues Thr308 and Ser473), GSK-3β (at Ser9, its inhibitory site) and CREB (at Ser133). Re-expression of CDKL5 restored AKT/GSK-3β signalling with a parallel restoration of NPC proliferation, survival and differentiation, confirming the direct implication of the kinase in the regulation of neurogenesis and neuronal maturation via AKT-GSK3β signalling (Fuchs et al., 2014).

A link between MeCP2 and cell proliferation has recently been identified in our laboratory (Bergo et al., 2015). In particular, we demonstrated that MeCP2 and its Y120 phospho-isoform localizes at the centrosome. This organelle is central for cell division, migration and differentiation in dividing and post-mitotic cells and an important regulator of cell proliferation. Indeed, both mouse embryonic fibroblasts (MEF) of *Mecp2*-null animals and silenced cells showed a reduction in cell growth. Moreover, down-regulation of *MeCP2* caused various centrosomal defects such as aberrant spindles, an increase in multinucleated cells and defects in microtubule nucleation. Even if CDKL5 disorder has recently been suggested to be

a distinct clinical entity, there are many data suggesting that CDKL5 and MeCP2 share molecular pathways: (i) the partially overlapping expression pattern (Rusconi et al., 2008), (ii) the ability of the two proteins to interact *in vivo* (Mari et al., 2005), (iii) the *in vitro* phosphorylation of MeCP2 by CDKL5 (Mari et al., 2005; Bertani et al., 2006, Williamson et al., 2012), (iv) the regulation of CDKL5 expression mediated by MeCP2 (Carouge et al., 2010), (v) common morphological and molecular defects (Amendola et al, 2014; Ricciardi et al., 2011; Fuchs et al., 2014; Armstrong, 2005). Altogether, the link of CDKL5 with MeCP2 and the ability of CDKL5 to regulate the balance between neuronal precursor proliferation/survival and differentiation during postnatal neurogenesis (Fuchs et al., 2014), suggest the implication of the kinase in regulating cell cycle progression; however, the molecular mechanisms through which CDKL5 influences this important cellular process are still unknown.

2. RESULTS

2.1 CDKL5 is required for the control of mitosis duration

To explore if CDKL5 might be implicated in regulation of cell cycle, we used HeLa cells cultures silencing CDKL5 for 60h and examined cell cycle progression at 37°C by time-lapse video light microscopy for 24h. These records revealed that cells interfered for Cdkl5 (iCdkl5) show a statistically significant longer prometaphase time (from the round-up to the chromosome segregation) t = 148.3 ± 91.34 min (n=73) versus 59.07 ± 33.64 min in iCtrl cells (n=73). In addition, iCdkl5 cells present a cytokinesis time (from cleavage furrow ingression to abscission) (t = 186.38 ± 78.39 min, n=66) higher than control cells (t = 139.1 ± 62.81 min, n=62) (Fig. 1A, 1B and Supplementary Movies S1 and S2). We did not observe any effect on cell viability or division failure in both iCtrl and iCdkl5 cells during the 24h imaging session. Consistent with prolonged prometaphase, ablation of CDKL5 induces a significative increase of mitotic index quantified through p-H3 immunostaining (Fig. 8 C, D). Moreover in order to understand if the ablation of CDKL5 could cause differences in the proliferation rate, we silenced HeLa cells for 60h in order to obtain efficient silencing (Fig. 8E); after this time, cells have been dissociated using trypsin, plated again in equal number and analysed at 24, 48 and 72h; as shown in figure 8F, we didn't observe any difference between proliferation rate of iCdkl5 cells respect to control siRNA. Summarizing, these data indicate that ablation of CDKL5 induces delay in mitosis progression without affecting proliferation rate.

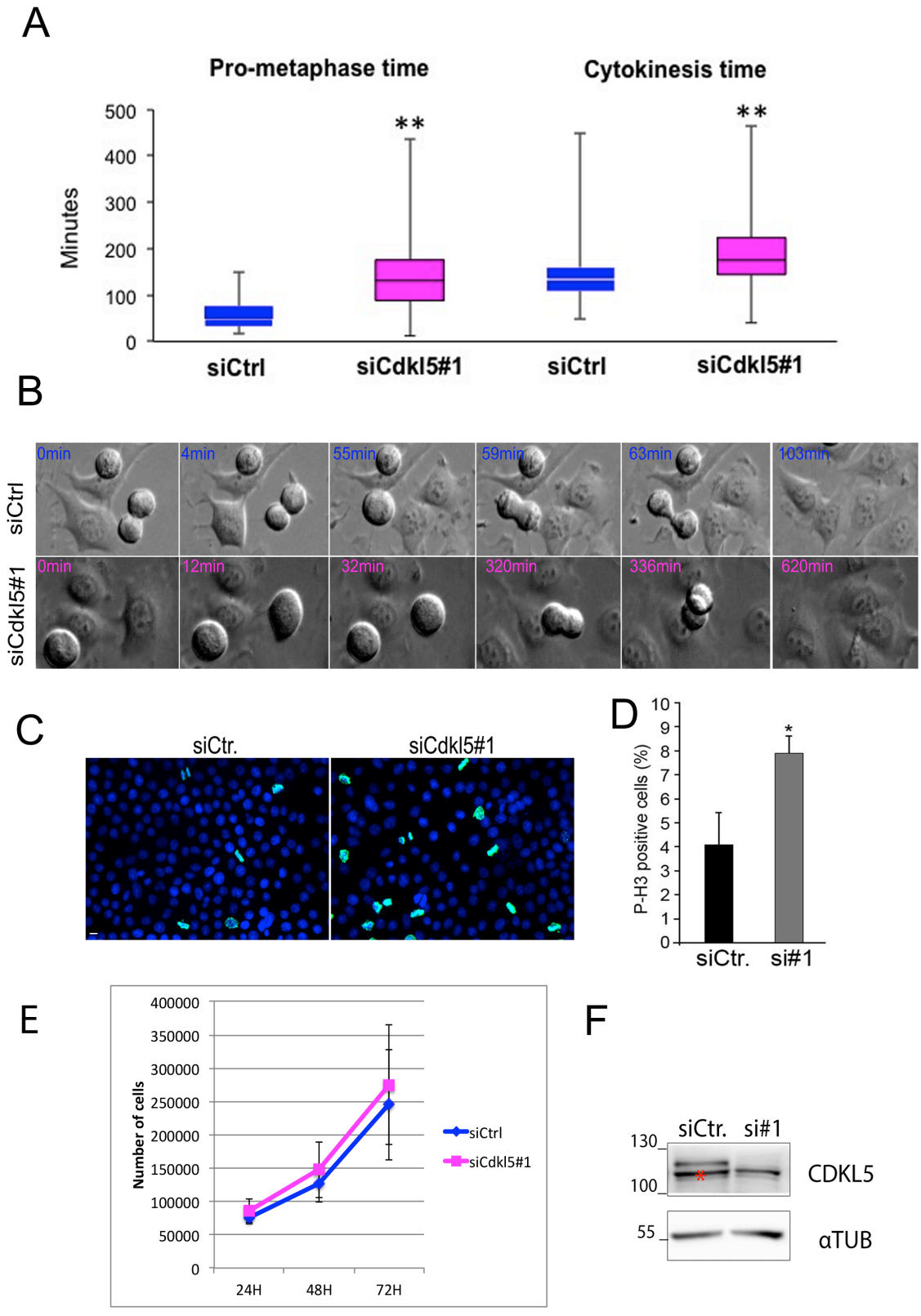

Figure 8 Loss of CDKL5 alters mitosis duration without affecting proliferation rate. A HeLa cells were transfected with Ctrl and Cdkl5#1 siRNA for 60h and analysed by time lapse video for 24h. In both cases, duration of the different phases of the mitosis and of the cytokinesis was measured. The duration of the indicated mitotic phases is reported in box plot graph (Whisker diagram). ***$p < 0.001$, Student's *t*-test. **B.** Still images related to Supplementary Movies S1 and S2. **C. D.** Asynchronously growing HeLa cells were analysed by IF for phosphorylated histone H3 (P-H3) 60 h after transfection with siRNA#1 targeting CDKL5, or a control siRNA (iCtr.). The percentage of P-H3 positive cells was calculated in in three independent experiments

counting approximately 100 cells in each experiment , $p < 0.05$, Student's *t* test. *Scale bars* = 10 μm **E.** Silenced CDKL5 and control HeLa cells were plated as described above and counted at the indicated time points ($n = 3$). **F**. Downregulation of CDKL5 at 60h after transfection was verified by WB using α-tubulin as loading control. The asterisk indicates a non-specific band.

2.2 CDKL5 is enriched at the centrosome

Prolonged prometaphase is often associated to an accumulation of cell division defects, usually caused by centrosome aberrations (Yang et al., 2008); this led us to investigate the subcellular localization of CDKL5. HeLa cells were thus stained for CDKL5 and γ-tubulin, which labels the centrosome and was used to distinguish the various mitotic phases. Permeabilization prior to fixation permitted us to better appreciate the well defined colocalization of endogenous CDKL5 with γ-tubulin from prometaphase till anaphase after which, we observed a reduction of its signal from centrosome and a contemporary increase in the midzone, in particulary at the midbody in the intracellular bridge (Fig. 9). In interphase, CDKL5 did not show any colocalization with the γ-tubulin positive centrosome, but it was present in typical dots within the nucleus corresponding, as previously described in literature, to nuclear speckles enriched in mRNA splicing factors (Ricciardi et al., 2009).

These data revealed for the first time new aspects of the subcellular localization of CDKL5 suggesting a role of the kinase in cell cycle process.

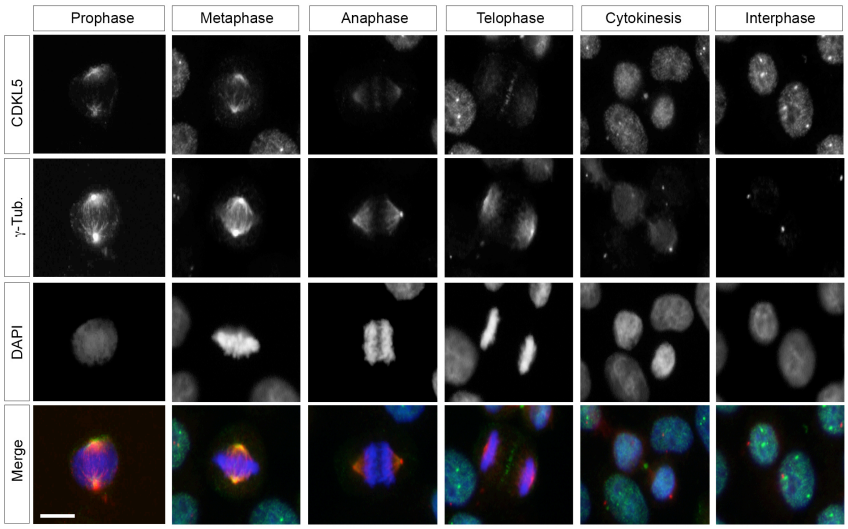

Figure 9 Localization of CDKL5 during cell cycle. HeLa cells were grown on coverslips, fixed, and costained with antibodies against CDKL5 (in *green*), γ-tubulin (γ-*tub*, *red*) and DAPI (*blue*) to visualize DNA. ($n > 3$). *Scale bars* = 10 μm.

In order to further validate the association of CDKL5 with centrosome, we performed experiments using different approaches. First, we confirmed by immunofluorescence the localization of endogenous CDKL5 at the γ-tubulin positive spots in different cell lines such as human lung fibroblasts (MRC5), monkey kidney fibroblasts (COS7), mouse neuroblastoma (Neuro-2A) and human neuroblastoma (SH-SY5Y) (Fig. 10A). In addition to endogenous CDKL5, we also expressed CDKL5 fused to the green fluorescent protein (GFP) in HeLa cells and, as can be seen in figure 10B, also the exogenous protein could be detected at the centrosome in mitotic cells. Finally, using a complementary biochemical approach, we isolated centrosomes from HeLa cells treated with nocodazole and cytochalasin D, to disrupt microtubules and actin cytoskeleton, by discontinuous sucrose gradient fractionation and subjected the isolated fractions to SDS-PAGE and Western blotting analysis. Fractions enriched for centrosomes were indicated by the presence of γ-tubulin. As shown in figure 10C, CDKL5 distribution in the fractions parallels that of γ-tubulin. The specificity of the result is demonstrated by the absence of any detectable signal in cells specifically depleted for CDKL5. Thus, biochemical data confirmed the presence of CDKL5 at the centrosome.

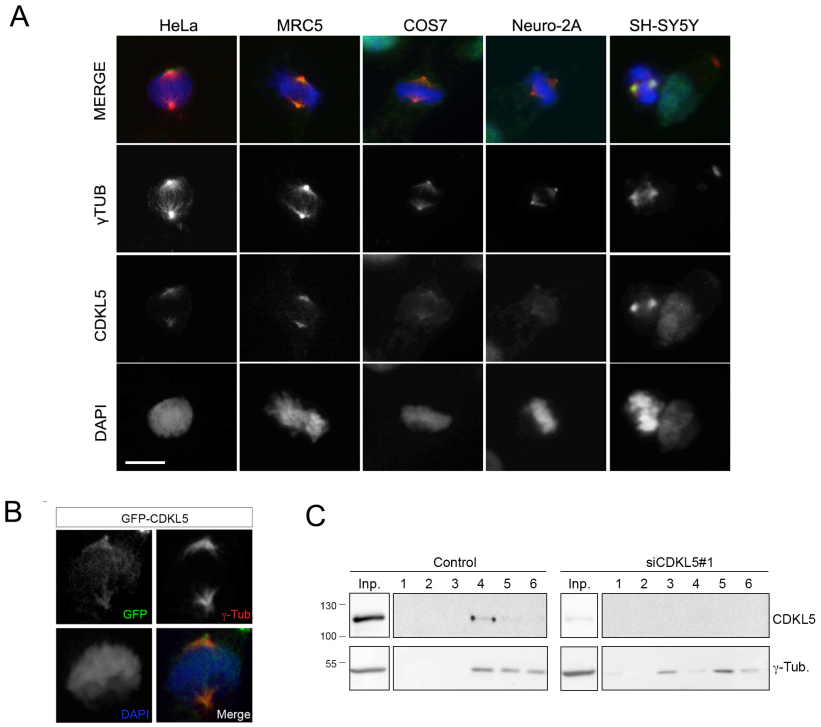

Figure 10. Endogenous and exogenous CDKL5 is targeted to the centrosome. A, MRC-5, COS-7, Neuro-2A and SH-SY5Y cells were immunostained with anti-CDKL5 (in *green*), anti-γ-tubulin (γ-*tub*, *red*) and labelled with DAPI (*blue*) to visualize DNA. ($n > 3$). *Scale bars* = 10 μm. **B.** HeLa cells expressing an exogenous GFP-

CDKL5 fusion protein (*green*) were analysed by immunostaining using anti-γ-tubulin (γ-*tub*, *red*) and DAPI (*blue*). **C.** HeLa cells were transfected with siCDKL5#1 or a control siRNA and three days post-transfection centrosomes were purified and the obtained fractions analysed by WB with anti-CDKL5 and anti-γ-tubulin. Fractions 1 and 6 are the bottom and top ones of sucrose gradient, respectively. Input signal corresponding to 0.6% of the extract loaded (n=3).

2.3 CDKL5 localizes at the midbody

We next proceeded analysing in more details the localization of CDKL5 in different cell lines during cytokinesis. We adopted the same strategy as above to validate the immunocytochemical association of CDKL5 with the midbody; to this aim, we performed immunostaining of different cell lines using α-tubulin or PLK1 as specific markers of the midbody bridge or stem body, respectively (Hu et al., 2012). As shown in figure 11A, endogenous CDKL5 was present at the stem body structure of the midbody of MRC5, COS7, and rat adrenal gland pheochromocytoma (PC12). The same localization was confirmed with exogenously expressed EGFP-CDKL5 (Fig. 11B).

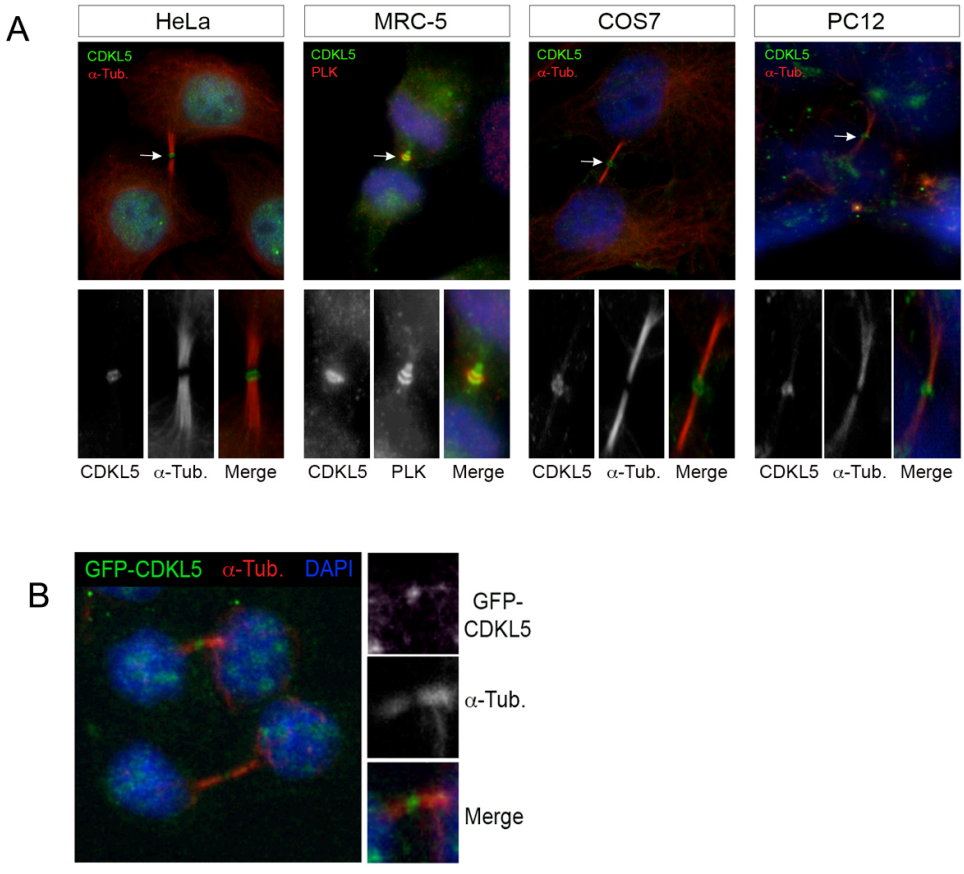

Figure 11 Endogenous and exogenous CDKL5 is targeted to the midbody A. HeLa, MRC-5, COS-7 and PC12 cells were immunostained with anti-CDKL5 (*green*), anti-α-tubulin (α-*tub*) or PLK1 (*red*) and labelled with

DAPI (*blue*) to visualize DNA. (n > 3). Arrows indicate the localization of CDKL5 in the central domain of the midbody (enlarged in the lower panels). **B.** HeLa cells expressing an exogenous GFP-CDKL5 fusion protein (*green*) were analysed by immunostaining using anti-α-tubulin (α-*tub*) and DAPI (*blue*). Insets show the magnified midbody.

2.4 Silencing of CDKL5 is associated with aberrant spindle pole geometry, chromosome alignment and micronucleation

Prolonged mitotic index, which is defined as the interval between nuclear envelope breakdown (NEB) and onset of anaphase, can be influenced by centrosome and/or chromosome amplification defects. Since we found that ablation of CDKL5 causes an increase in the time spent in mitosis and that CDKL5 is a component of the centrosome, we decided to analyse whether CDKL5 influences mitotic spindle assembly. To explore this, we transfected HeLa cells with two specific siRNAs silencing CDKL5 with high efficiency (siCdkl5#1, siCdkl5#2; figure 12A) and analysed spindle geometry 60h post-silencing using α-tubulin to highlight the mitotic spindle. The analysis revealed that >50% cells interfered for Cdkl5 show a statistically significant loss of mitotic spindle pole integrity; among them, there is an increased (about 30% in iCdkl5 cells versus about 12% in iCtrl cells) incidence of cells with multipolar spindles (Fig. 12B-D). This phenomena correlate with the failure of chromosome alignment in iCdkl5 cells respect to control (Fig. 12E). Interestingly, DAPI staining in HeLa cells iCdkl5 permitted to observe an increased number of micronuclei which are extranuclear bodies that are formed during mitosis from lagging chromosomes (Hayashi et al., 2013) (Fig. 12F).
Further, we decided to analyse the same phenotype in MRC5; also in this cell line, the depletion of Cdkl5 caused an increase in aberrant spindle formation and failure of chromosome alignment (Fig. 12 G-M).

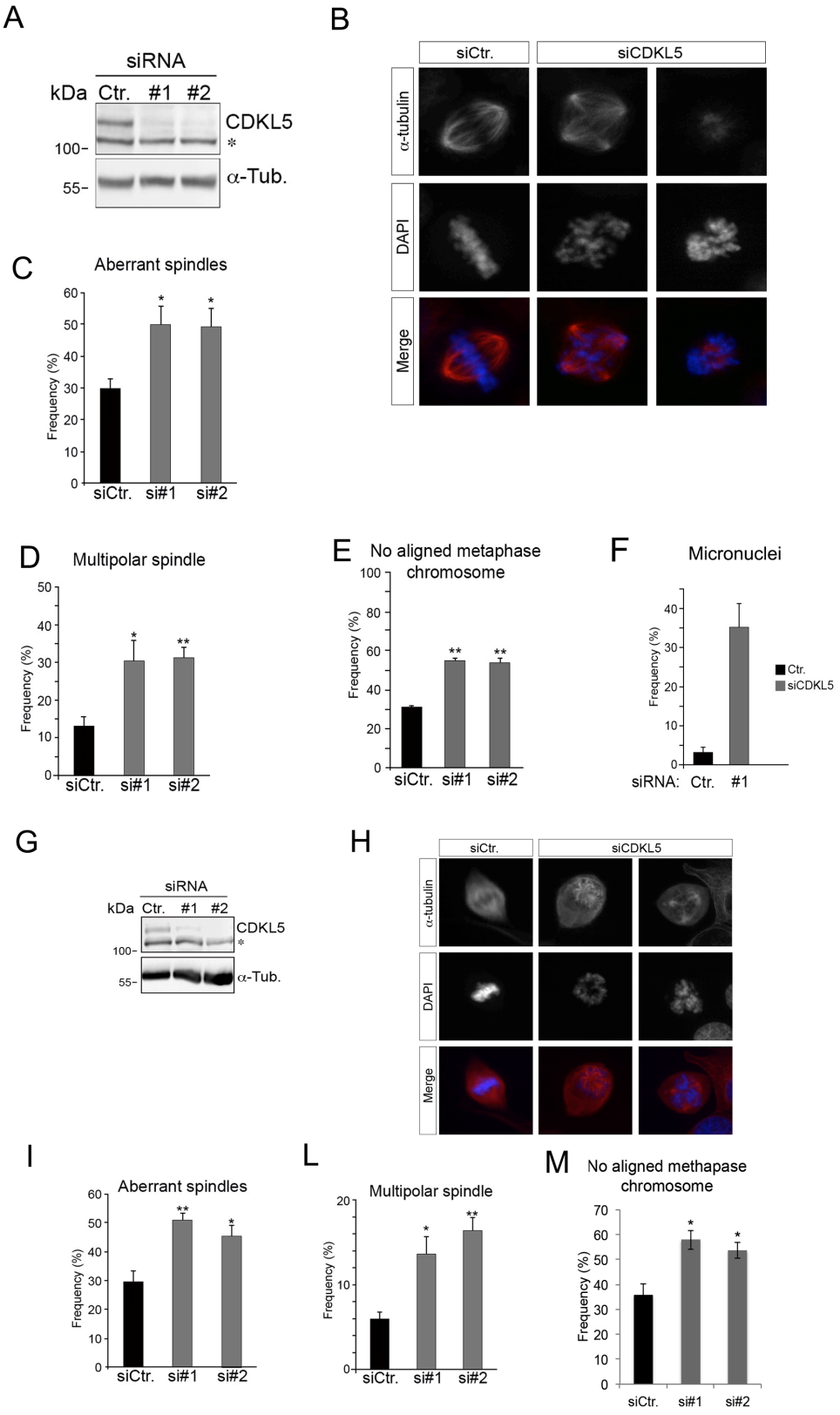

Figure 12 Silencing of CDKL5 is associated with aberrant spindle pole geometry, chromosome alignment and micronuclei formation. A. WB showing silencing of CDKL5 expression in HeLa cells with two distinct siRNAs using α-tubulin as loading control. The asterisk indicates a non-specific band. **B**. Representative images of HeLa cells treated as in A after staining against α-tubulin (α-tub) (red) and with DAPI (blue). **C.** Graph showing the average of aberrant spindles of three independent experiments counting >100 cells per experiment; (mean ±S.E, unpaired t-test). **D.** The average of cells with multipolar spindles was

determined in three independent experiments (mean ±S.E, unpaired t-test). **E.** Graph showing the average of metaphase cells with abnormally aligned chromosomes in two independent experiments counting >240 cells per experiment (mean ±S.E, unpaired t-test). **F.** Graph showing the average of microluclei formation. **G.** WB showing silencing of CDKL5 expression in MRC5 cells with two distinct siRNAs using α-tubulin as loading control. The asterisk indicates a non-specific band. **H.** Representative images of HeLa cells treated as in G after staining against α-tubulin (α-tub) (red) and with DAPI (blue). **I.** Graph showing the average of aberrant spindles of three independent experiments counting >137 cells per experiment; (mean ±S.E, unpaired t-test). **L.** The average of cells with multipolar spindles was determined in three independent experiments (mean ±S.E, unpaired t-test). **M**. Graph showing the average of metaphase cells with abnormally aligned chromosomes in two independent experiments counting >227 cells per experiment (mean ±S.E, unpaired t-test).

The direct involvement of CDKL5 in regulating spindle pole geometry and chromosome segregation was suggested by the fact that both siRNAs targeting the kinase caused similar defects; nevertheless, we excluded that the observed phenotype was due to off-target effects by performing rescue experiments in which a siRNA-resistant CDKL5 cDNA was introduced into silenced cells. Vectors expressing CDKL5 and GFP from a bicistronic cassette, or GFP alone as control, were introduced into silenced cells and CDKL5 expression and mitotic spindle organization analysed by WB and immunostaining (Fig. 13). As above, a significant number of cells silenced for CDKL5 were characterized by aberrant mitosis with respect to control cells; importantly, however, no significant difference could be observed when CDKL5 was re-expressed.

Taken together, these data show that CDKL5-depleted cells fail to efficiently align chromosomes to the metaphase plate, resulting in a prolonged prometaphase and in accumulation of cell division defects, usually associated to centrosome aberrations.

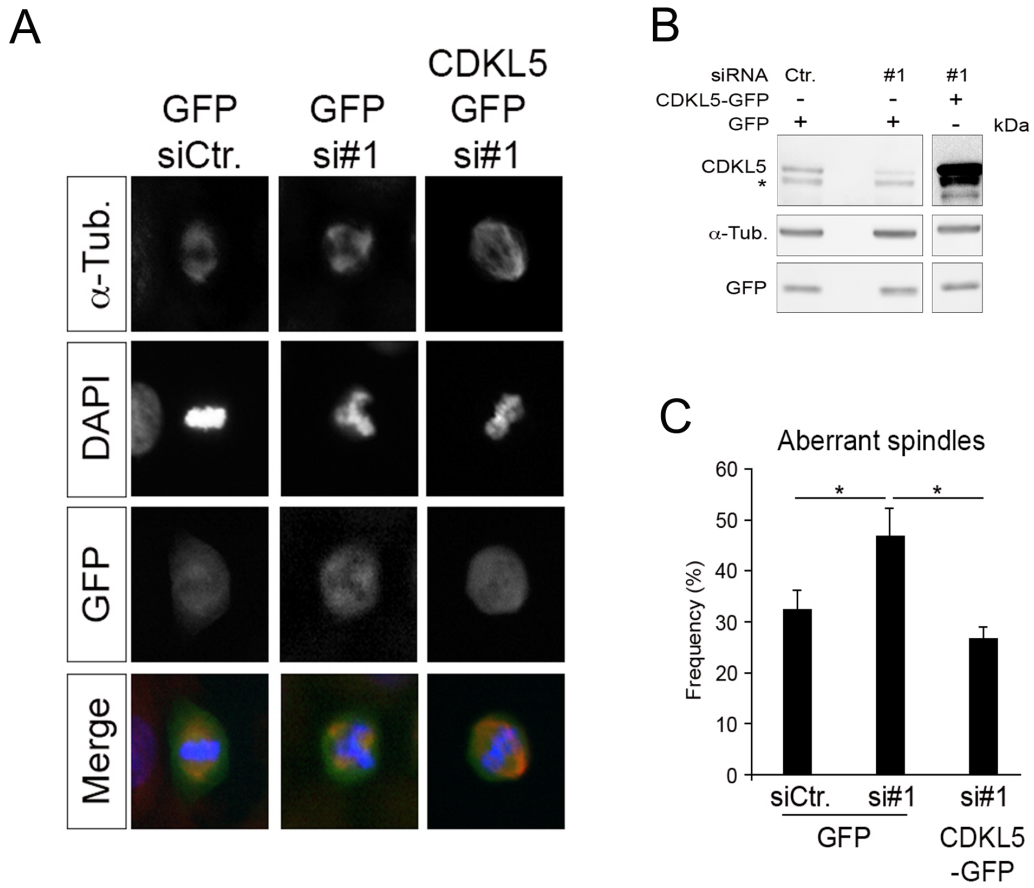

Figure 13 Mitotic defects can be rescued by the reintroduction of CDKL5. A. Representative images of spindle pole geometry in GFP-positive cells (green) stained against α-tubulin (red) and with DAPI (blue). CDKL5 was expressed in HeLa cells by transfection of a bicistronic vector expressing also GFP four days post-silencing. **B**. CDKL5 levels were determined by WB using α-tubulin as loading control. **C.** The presence of aberrant spindle poles in GFP-positive cells was quantified in three independent experiments counting >70 cells per experiment (mean ±S.E, unpaired t-test).

2.5 CDKL5 localizes to the centrosome of neuronal progenitors

We next examined the expression of CDKL5 in neuronal precursors cells cultures (NSC) derived from the developing mouse brain (E14). Cells were maintained as undifferentiated neurospheres in the presence of basic FGF (bFGF) and EGF, and were labelled, as above, with CDKL5 and γ-tubulin antibodies. Immunofluorescence analysis revealed the colocalization of CDKL5 and centrosome also in NSC cells (Fig. 14); conversely the cell lines previously analysed, where CDKL5 localized at the centrosome in mitotic phases but not in interphase, in NSC cells the kinase remains anchored to centrosome throughout

the whole cell life. Since centrosome is an important cytoskeleton structure that governs many process as cell division, migration and differentiation (Azimzadeh et al., 2007; Bettencourt- Dias et al., 2007; Doxsey et al., 2005; Nigg et al., 2009), these data suggest a possible implication of CDKL5 in these cellular mechanisms via centrosome dependent signalling.

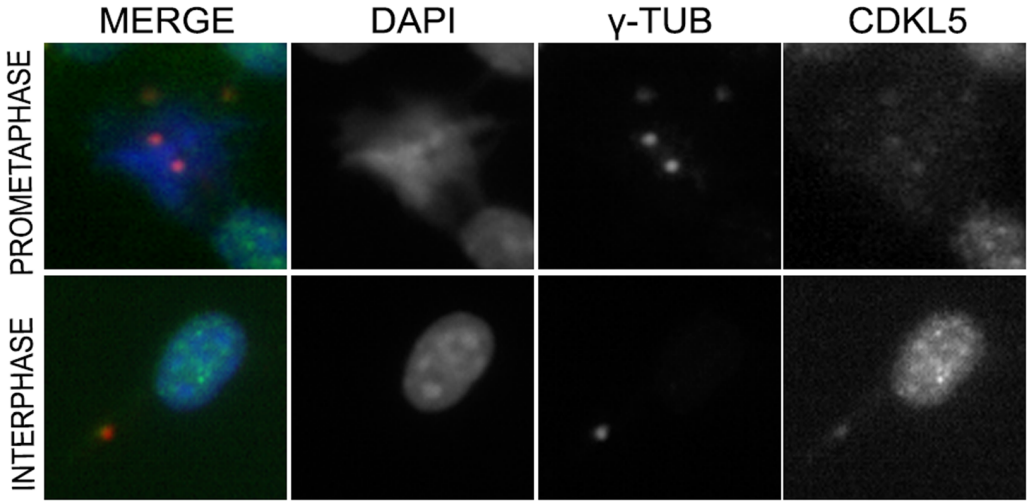

Figure 6 CDKL5 localizes at the centrosome of neurospheres cells. NSC cells were grown on coverslips, fixed, and co-stained with antibodies against CDKL5 (in *green*), γ-tubulin (γ-*tub*, *red*) and DAPI (*blue*) to visualize DNA.

2.6 CDKL5 influences microtubule organization

Thanks to the ability of centrosome to provide a structural hub for the organization of the microtubule (MT) array, it represents a central component of the cytoskeleton. Several diseases of brain development have been linked to defects in centrosome and MT-regulating proteins (Kuijpers et al., 2011). We therefore found it challenging to explore whether CDKL5 might regulate cytoskeletal dynamics and examined the effect of CDKL5 depletion on microtubule organization. To this aim, COS7 cells were silenced for CDKL5 expression for three days where after the silencing efficiency was verified by Western blot (Fig. 15A). As shown in figure 15B, down-regulation of CDKL5 caused a marked change in the microtubule organization. Indeed, the intracellular distribution of microtubules in a circular-like shape that is evident in control cells was less pronounced in cells with reduced levels of CDKL5.

Given the influence of CDKL5 on microtubule organization and since our data demonstrate a role of CDKL5 in centrosome maturation and mitotic spindle assembly, we wondered if the kinase could play a role in regulating microtubule nucleation. To test this possibility, we transfected COS7 cells with CDKL5 siRNAs and used nocodazole to transiently depolymerize microtubules. The formation of nascent microtubules was analysed 30 min after nocodazole washout. As shown by α-tubulin staining in the upper panel of figure 15C, 3h of nocodazole was sufficient to depolymerize microtubules both in control and CDKL5 depleted cells. After 30 minutes of recovery in fresh medium, although microtubule nucleation from the centrosome could still occur in iCdkl5 cells (Fig. 15C), the newly formed MT network was severely affected in terms of the spatial array of α-tubulin filaments. Indeed, microtubules were randomly distributed in CDKL5 silenced cells, while in control cells they were organized in a regular aster-like distribution. Quantification of the aster area, marked by α-tubulin, revealed a significant reduction of this parameter (Fig. 15D). Altogether, these data demonstrate that CDKL5 influences the distribution of microtubules without affecting the polymerization process.

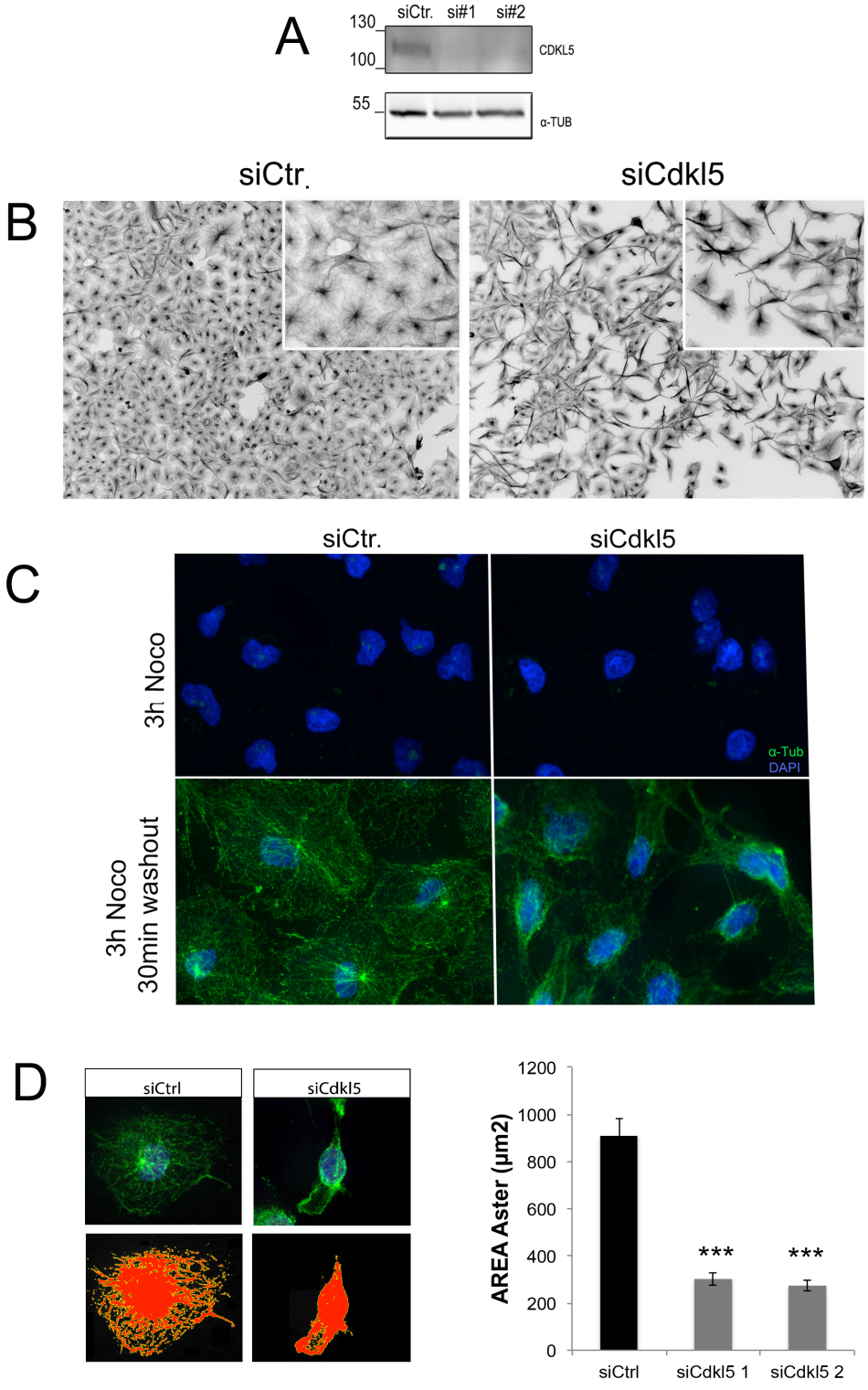

Figure 15 CDKL5 down-regulation affects microtubule distribution. A. WB showing the expression level of CDKL5 in COS7 cells three days post-transfection with control and CDKL5 siRNAs; α-tubulin (α-tub) was used as loading control. **B.** COS7 cells treated as in *A*, were fixed and stained for α-tubulin (α-tub, green) to analyse microtubule organization and with DAPI (blue). Insets show high-magnification images of microtubule array. **C.** COS7 cells treated as in *A* were exposed to the microtubule-destabilizing drug nocodazole 10 µg/ml (noco) for 3 h (top). Microtubule regrowth was tested by releasing the cells in fresh medium for 30 min (bottom), where after they were fixed and stained with anti α-tubulin (α-tub) (*green*). Nuclei were stained with DAPI (*blue*). **D.** Representative image showing method for calculating aster area using Image J software

(left). On the right, the quantification of aster area after 30-min release upon nocodazole treatment is shown (n > 100 cells in three independent experiments, mean ± S.E.). ***, p < 0.001; Student's t test.

2.7 IQGAP1 is a novel interactor of CDKL5

The knowledge of proteins interacting with CDKL5 is instrumental to understand the functions and the molecular pathways associated with this kinase. For this reason, a two-hybrid screening had previously been performed in our laboratory in which the C-terminal region of hCDKL5 (amino acids 299-1030 of the 107 kDa isoform) was used as bait to screen a human adult brain cDNA library. 171 interacting clones were obtained, of which IQGAP1 caught our attention. IQGAP1, an effector of active Rac1/Cdc42 (Kuroda et al., 1996; Fukata et al., 2001), is a scaffold protein involved in the formation of complexes that regulate cytoskeletal dynamics through actin and microtubule organization (Malarkannan et al., 2012). The surface of IQGAP1 contacting CDKL5 is contained within amino acids 82-357, as illustrated in figure 16A. The interaction between CDKL5 and IQGAP1 was further supported by co-immunoprecipitation experiments, in which an anti-IQGAP1 antibody, but not rabbit IgGs, precipitated CDKL5 from P11 mouse-brain extracts (Fig. 16B). The same experiments were repeated in HeLa cells and by subsequent Western blot analysis we could detect CDKL5 as co-precipitating with IQGAP1, but not with rabbit IgGs (Fig. 16C). Finally, we also performed co-immunoprecipation assays with HeLa cells expressing exogenous Myc-CDKL5; 24 h after transfection, when cells expressed significant amounts of Myc-CDKL5, total cell lysates were harvested and incubated with an anti-Myc agarose resin. Western blot analysis of the immunocomplexes revealed that IQGAP1 was efficiently co-immunoprecipitated when cells expressed Myc-CDKL5 but not from a control lysate expressing Myc alone (Fig. 16D). Altogether, these results identify IQGAP1 as a novel interactor of CDKL5.

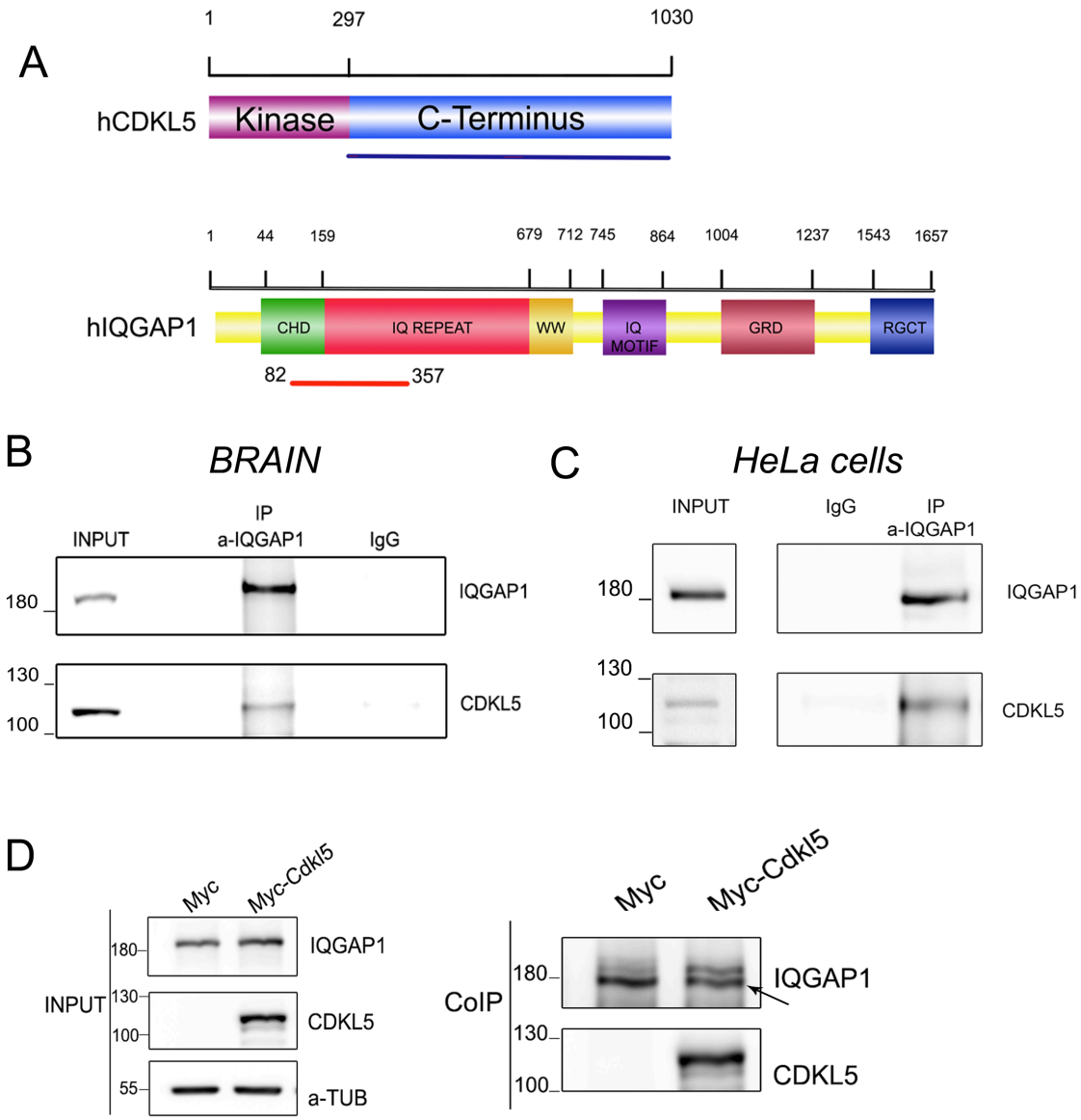

Figure 16 CDKL5 interacts with IQGAP1 *in vivo*. A yeast two-hybrid screening identified IQGAP1 as a CDKL5 interacting protein. The C-terminal region of hCDKL5, spanning amino acids 299-1030, was used as bait (top, blue bar). The diagram to the bottom represents IQGAP1 with its six domain: questa parte non è meglio metterla nel testo? the calponin homology (CH) domain binds the chemokine receptor, CXCR2, and regulates the actin cytoskeleton by binding N-WASp and polymerized filamentous actin (F-actin). IQ-Repeats consists of six coiled-coil regions. Tryptophan-containing (WW) domains recruit Erk1/2. The isoleucine/glutamine-containing (IQ) domain is a binding domain for multiple proteins that include components of MAPK signalling. The Ras-GAP domain (GRD) does not function as a GTPase Activating Protein (GAP) but does interact with small GTPases Cdc42, Rac1, and TC10. The Ras-GAP C-terminus domain (RGCT) interacts with microtubule-binding proteins CLIP170 and Clasp2, as well as membrane-resident proteins such as β-catenin, E-cadherin, and APC. **B.** Co-immunoprecipitation of P11 mouse brain lysates with anti-IQGAP1 antibodies. Rabbit IgGs were used as negative control. The immunoprecipitates and inputs (5% of the brain lysates) were analysed by immunoblotting for CDKL5 and IQGAP1 (n=2). **C.** Co-immunoprecipitation of HeLa cell lysates with anti-IQGAP1 antibodies. Rabbit IgGs were used as negative control. The immunoprecipitates and inputs (5% of total lysates) were analysed by immunoblotting for CDKL5 and IQGAP1 (n=3). **D.** Co-immunoprecipitation of HeLa cells overexpressing Myc and Myc-CDKL5. The immunoprecipitates and inputs (5% of total lysates) were analysed by immunoblotting for CDKL5 and IQGAP1 (n=1). Arrow indicates an unspecific signal.

2.8 CDKL5 and IQGAP1 co-localize at the cell cortex and at the centrosome

We further proceeded considering whether a common localization of CDKL5 and IQGAP1 could be detected within cells. The capacity of IQGAP1 to coordinate cell polarization and migration has in the past been associated with its localization at the leading edge (Fukata et al., 2002; Watanabe et al., 2005). Likewise, CDKL5 has previously been detected at the cell cortex upon Rac1 activation (Chen et al., 2010), even if the biological meaning of this localization has to be further clarified. We proceeded with immunofluorescence experiments using exogenously expressed GFP-IQGAP1. As shown in figure 17A, endogenous CDKL5 and GFP-IQGAP1 presented a common localization at the cortex of COS7 cells in correspondence with the lamellipodia, which are actin-rich membrane protrusions that drive cell migration (Krause et al., 2014).

Interestingly, we also detected endogenous IQGAP1 at the centrosome both by immunofluorescence as well as through the biochemical centrosome extraction of HeLa cells described above. Indeed, in this assay we were able to detect both CDKL5 and IQGAP1 in sucrose gradient fractions enriched for the centrosome marker γ-tubulin (Fig 17B; C).

The common localization of CDKL5 and IQGAP1 at the centrosome and at the cell cortex suggests that the two proteins may participate to some related functions in these sites.

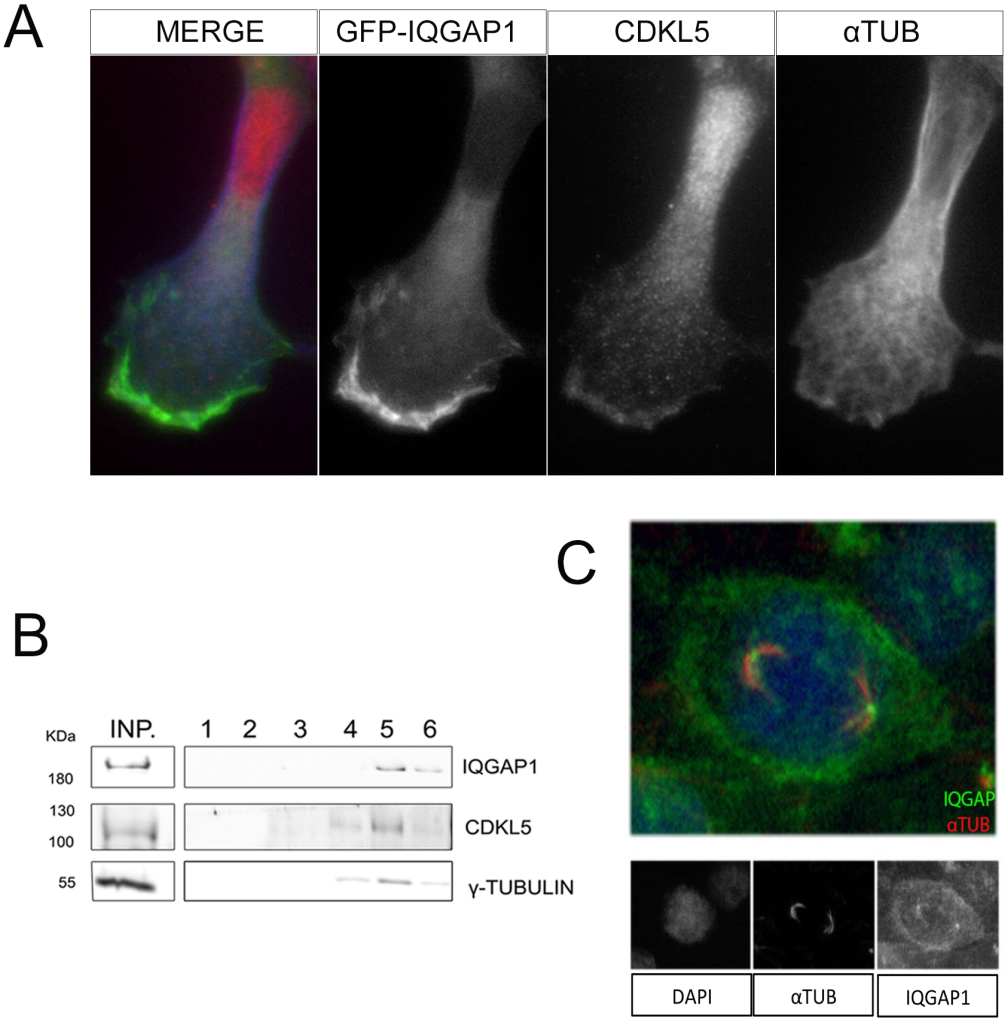

Figure 17 CDKL5 and IQGAP1 co-localize at the cell cortex and at the centrosome. A. Immunofluorescence of COS7 cells transfected for 24h with pEGFP-IQGAP1 (green) and stained for CDKL5 (red) and α-tubulin (blue). **B.** WB showing the presence of IQGAP1, CDKL5 and γ-tubulin in fractions of purified centrosomes. Fractions 1 and 6 are the bottom and top ones of the sucrose gradient, respectively (n=3). **C.** COS7 cells were immunostained with anti-IQGAP1 (in green), anti-α-tubulin (α-tub, red) and labelled with DAPI (blue) to visualize DNA.

2.9 IQGAP1 changes its localization at the leading edge in CDKL5 depleted cells

To analyse whether CDKL5 is required for the accumulation of IQGAP1 at the polarized leading edge during cell migration we performed a wound-healing assay in which cell migration is induced by generating a "wound gap" in a cell monolayer. A scratch was generated in confluent COS7 cells (T0, time zero) transfected with control and CDKL5 siRNAs and migrating cells were analysed 5h later (T5h). Consistently with our previous data performed in HeLa cells (data not shown), the ablation of CDKL5 caused a reduction in cells migration (Fig. 18A): in fact, the

quantification of the distance between the two faces of the wound (Fig. 18B) showed that while control cells covered 60% of the wound between T0 and T5h, CDKL5 silenced cells after 5h presented a “wound occupancy” comparable to T0 (the apparent increase of the distance after 5h in iCdkl5 cells was due to manually differences during the generation of the wound). Moreover, control cells showed a typical polarized morphology, with a single leading edge facing the wound where IQGAP1 (green) accumulated and co-localized with F-actin (red); on the contrary, upon CDKL5 silencing the actin meshwork was less evident and the accumulation of IQGAP1 at the leading edge was compromised. The intensity quantification of the IQGAP1 signal with Image J along a segment of 10 μm from the cell cortex towards the cytoplasm (figure 18B,C) showed an opposite trend in control and siCdkl5 cells: in fact, in control cells the IQGAP1 signal peaked in correspondence of the cell cortex and decreased towards the cytoplasm whereas in iCdkl5 cells the signal reached its maximum intensity in the cell lumen and declined towards the periphery. Thus, CDKL5 seems to be necessary for the correct localization of IQGAP1 at the leading edge, but we cannot say whether this depends on the direct interaction of the two proteins or if the ablation of CDKL5 induces per se a deregulation of the actin meshwork causing the delocalization of IQGAP1. Further studies using siRNA resistant derivatives of CDKL5 lacking the IQGAP1 interaction domain, will be useful to clarify this point.

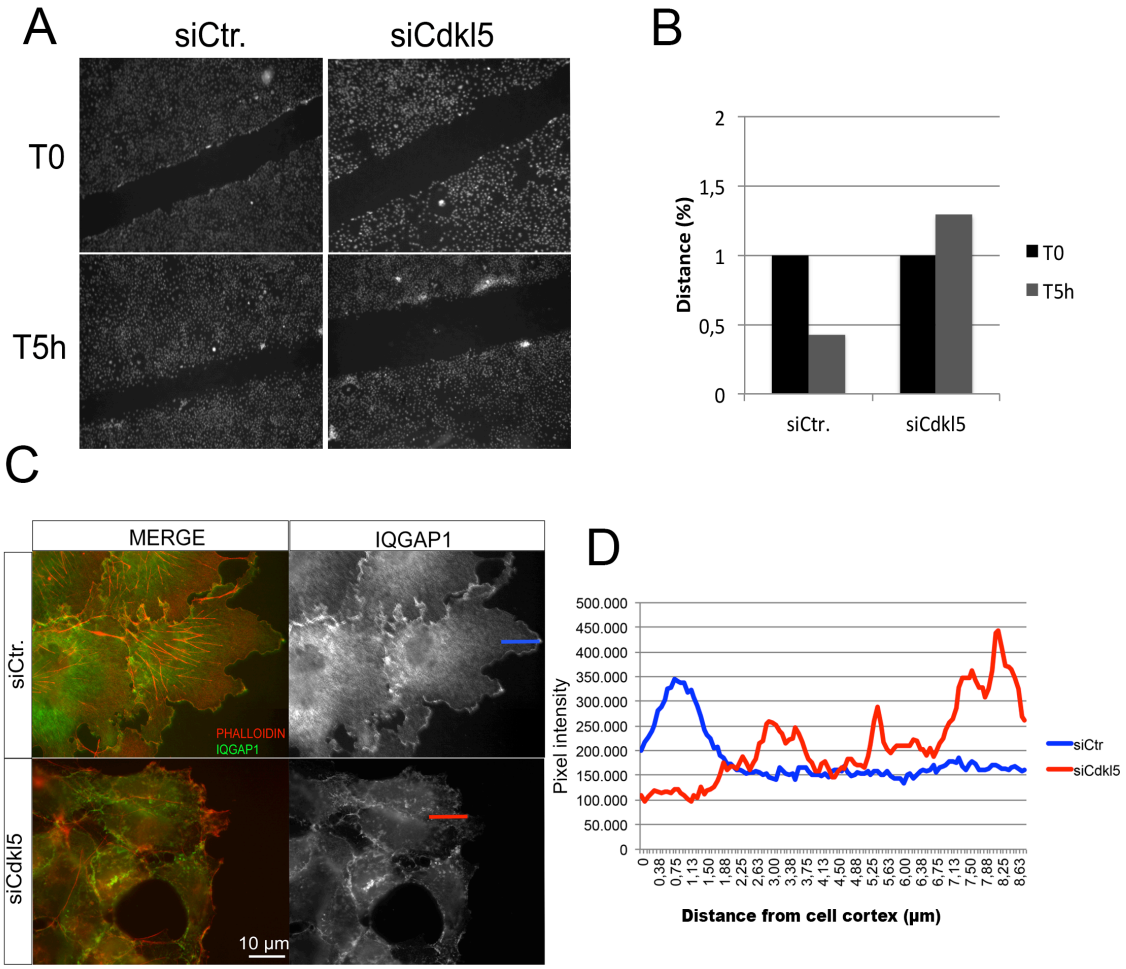

Figure 18 IQGAP1 changes its localization at the leading edge in CDKL5 depleted cells. A. Migration of control and CDKL5 silenced COS7 cells into a scratch wound was monitored by following a time-course immunofluorescence. Cells were fixed and stained with DAPI immediately (T0) after the scratch and 5h (T5H) later to evaluate the migration ability of cells into the wound. **B.** A quantitative analysis of the migration assay was done using the ImageJ software *n*=2. **C.** Representative images of wound-healing assays. COS7 cells were transfected with control or CDKL5 siRNAs and after three days a scratch was performed with a pipette tip. After 5 h cells were fixed and immunostained with anti-IQGAP1 (green) and phalloidin (red) **D.** Plot profile showing the pixel intensity of the IQGAP1 signal from the cell cortex towards the inner cell area between iCtr. (blue line) and iCdkl5 cells (red line).

2.10 Iqgap1 down-regulation alters the distribution of microtubules nucleated at the centrosome

In order to understand if CDKL5 and IQGAP1 belongs to a common molecular pathway implicated in the maintenance of cell shape, we repeated the microtubule nucleation experiment in COS7 three days after silencing of IQGAP1 (siIqgap1; Fig. 12A). As shown in figure 19B, nocodazole treatment followed by thirty minutes of recovery inhibited the capacity of cells interfered for IQGAP1 to regenerate a radial

array, determining as in the case of CDKL5 deficient cells, a significative reduction of total aster area.

Altogether, these results show that both CDKL5 and IQGAP1 are required to maintain correct cytoskeletal microtubules dynamics.

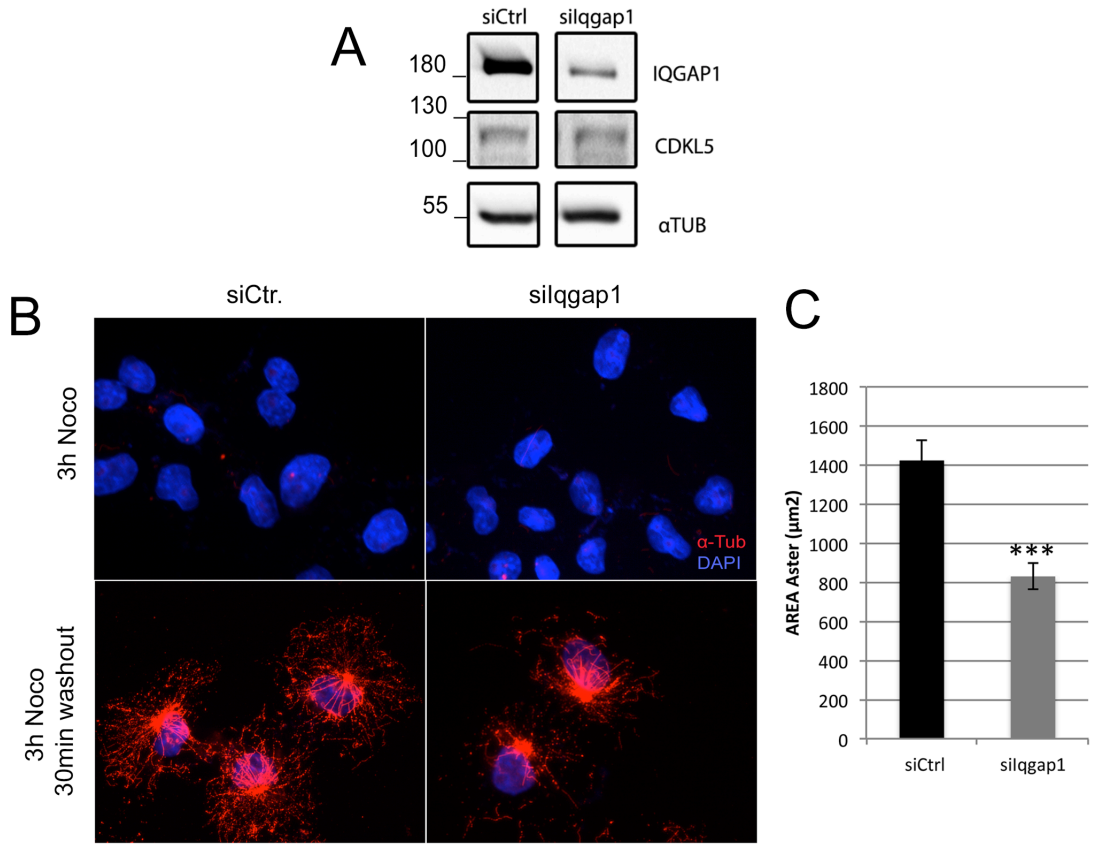

Figure 19 Downregulation of IQGAP1 affects microtubule distribution. A. WB showing expression level of IQGAP1 in COS7 cells transfected for three days with control and IQGAP1 siRNA; α-tubulin (α-tub) was used as loading control. **B.** COS7 cells treated as in A were exposed to the microtubule-destabilizing drug nocodazole 10 µg/ml (noco) for 3 h (top). Microtubule regrowth was analysed by releasing the cells in fresh medium for 30 min (bottom), where after they were fixed and stained with anti α-tubulin (α-tub) (*red*) and with DAPI (*blue*). **C.** Quantification of aster area after 30 min release upon nocodazole treatment (n = 50 cells, mean ± S.E.). ***, $p < 0.001$; Student's t test.

2.11 Down regulation of CDKL5 reduces the binding of IQGAP1 to Rac1 and CLIP170

In fibroblasts, MT minus ends are anchored to the microtubule organizing centre (MTOC), whereas MT plus ends are directed to the cell periphery and continually alternate between two phases: elongation and shrinkage (dynamic instability). Dynamic instability is thought to enable MT to search for and capture special sites

in the cell cortex through plus-end-binding proteins (+TIPs) that accumulate at the plus-ends of growing microtubules and play crucial roles in sensing cortical capture sites. Activated Rac1 binds IQGAP1 enhancing the interaction between IQGAP1 and CLIP170, one of the +TIPs (Fukata et al., 2002). Knocking down IQGAP1 by RNA interference decreases the number of immobilized CLIP170 complexes at the leading edge of polarized fibroblasts, leading to a reduced interaction between the cell cortex and the microtubule meshwork and causing the alteration of a polarized MT array (Watanabe et al., 2004).

Considering the central role of IQGAP1 in microtubule organization together with the cytoskeletal defects generated by the ablation of CDKL5 described above, we decided to investigate the relationship between IQGAP1, Rac1 and CLIP170 in cells depleted for CDKL5. Thus, we first immunoprecipitated IQGAP1 from HeLa cells silenced for three days for CDKL5 and analysed by Western blot the presence of Rac1 in the pellet. As shown in figure 20A, Rac1 was easily precipitated together with IQGAP1 from control cells, but when CDKL5 was down-regulated with either of two siRNAs, the amount of Rac1 bound by IQGAP1 was reduced approximately 60% and 40% with siCDKL5#1 and siCDKL5#2, respectively (Fig. 20B). We next evaluated the amount of IQGAP1 co-immunoprecipitated with CLIP170 from silenced HeLa cells. Interestingly, the ablation of CDKL5 with both siRNAs reduced the binding of the two proteins by nearly 50% (Fig. 20 C, D). Altogether, these data indicate that CDKL5 influences the ability of IQGAP1 to interact with Rac1 and CLIP170 likely alerting the MT array.

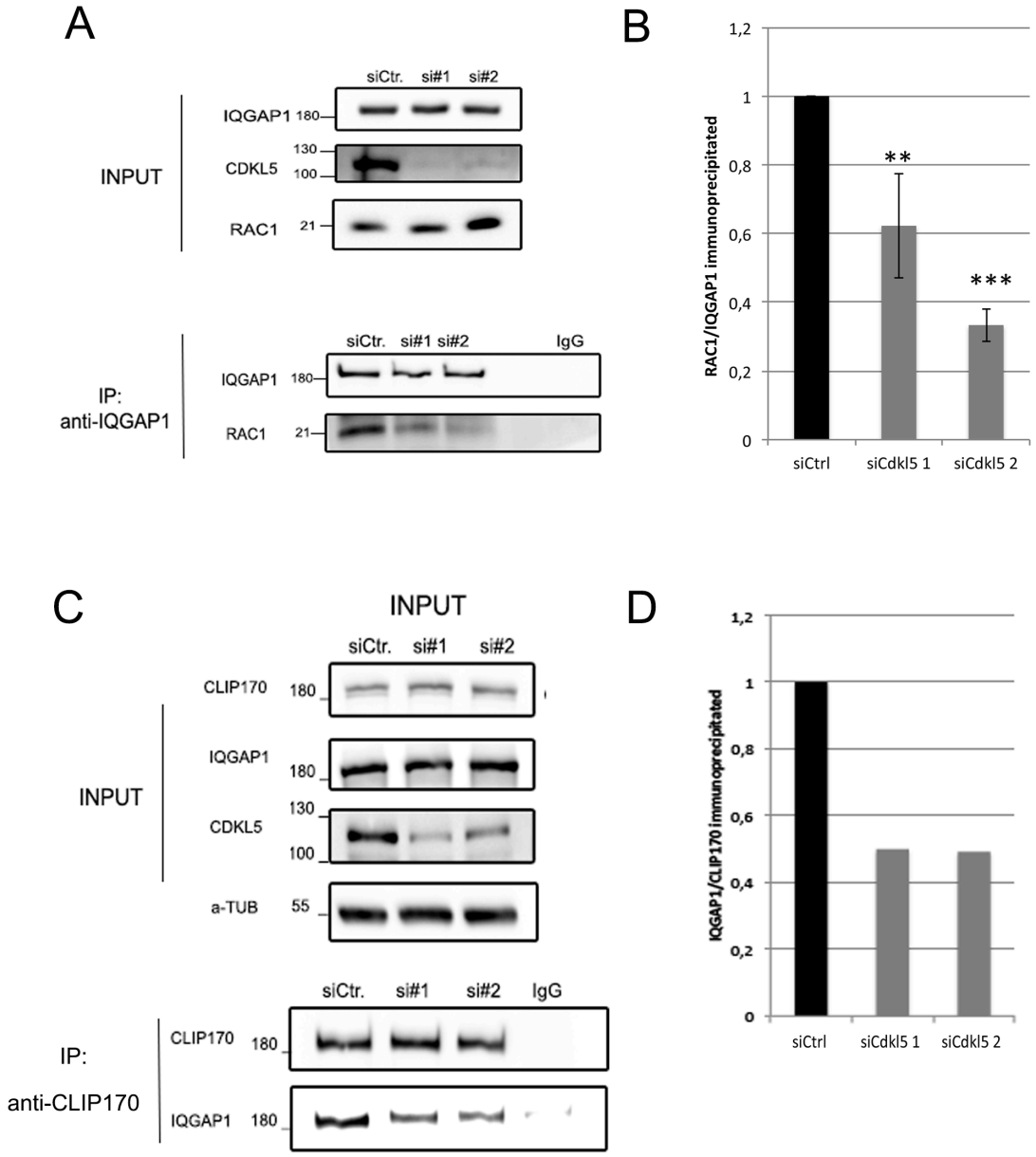

Figure 20 Down-regulation of CDKL5 reduces the binding of IQGAP1 to Rac1 and CLIP170. A. Co-immunoprecipitation of HeLa cell lysates with anti-IQGAP1 antibodies. HeLa cells were interfered for three days with CDKL5 siRNAs (#1 and #2). Rabbit IgGs were used as negative control. The immunoprecipitates and inputs (5% of the brain lysates) were analysed by immunoblotting for IQGAP1 and Rac1. **B.** Quantification of the data shown in *A,* Rac1 co-immunoprecipitation (co-IP) intensity was normalized to IQGAP1 immunoprecipitation (n=5 for siCdkl5#1 and n=4 for siCdkl5#2, mean ± S.E.). **, $p < 0.01$ ***, $p < 0.001$; Student's *t* test. **C**. Coimmunoprecipitation of HeLa cells treated as in A with anti-CLIP170. The immunoprecipitates and inputs (5% of the brain lysates) were analysed by immunoblotting for CLIP170 and IQGAP1. **D.** Quantification of the data shown in *C,* IQGAP1 co-immunoprecipitation (co-IP) intensity was normalized to CLIP170 immunoprecipitation (n=1 for siCdkl5#1 and n=1 for siCdkl5#2).

3. DISCUSSION

3.1 CDKL5 localizes at the centrosome and influences cell division and spindle pole assembly

Mutations in the *CDKL5* gene, located on Xp22, have been described as the cause of the "early seizures variant" of classic RTT syndrome (Weaving et al., 2004), also known as the Hanefeld variant (Hanefeld, 1985). Many scientific pieces of evidence suggest an inter-talk between *CDKL5* and *MECP2* (Mari et al., 2005, Lin et al., 2005, Bertani et al., 2006; Carouge et al., 2010), which is the main cause of classic RTT. However, the increasing number of patients mutated in *CDKL5* and the expanded knowledge of RTT led to consider CDKL5 disorder separated to RTT (Neul et al., 2010; Fehr et al., 2013). CDKL5 disorder is a neurological condition characterized in the majority of cases by the onset of intractable seizures within three months of age, severely impaired gross motor, language and hand function skills and some dysmorphic facial features such as prominent and/or broad forehead, high hairline, relative midface hypoplasia, deep-set but large appearing eyes and infra-orbital shadowing (Fehr et al., 2013). Despite the evident role of CDKL5 for the correct development of the nervous system, the association of this gene with human pathologies is relatively recent, dating back only to 2003 (Kalscheuer et al., 2003); consequently, the knowledge on CDKL5 functions are constantly evolving.
CDKL5 is a kinase that shuttles between the nucleus and the cytoplasm (Rusconi et al., 2008) where, thanks to specific interactors, it is able to orchestrate important cellular functions. In the nucleus, CDKL5 seems to have a role in the regulation of gene expression through its interaction with DNA methyltransferase 1 (DNMT1) (Kameshita et al., 2008) and MeCP2 (Mari et al., 2005; Bertani et al., 2006); moreover, it associates with nuclear speckles involved in RNA splicing (Ricciardi et al., 2008). In the cytoplasm, CDKL5 seems to have a role in the activation and maintenance of synaptic activity (La Montara et al., 2015), in the regulation of cytoskeleton rearrangements through the interaction with Rac1, (Chen et al., 2010), in the preservation of synaptic strength and stability via NGL1 phosphorylation and interaction with PSD95 (Ricciardi et al., 2012; Zhu et al., 2013) and in the synaptic vesicle recycling through Amph1 interaction (Sekiguchi

et al., 2013). The morphological defects observed *in vitro* in interfered neurons have recently been confirmed also *in vivo* thanks to the development of two *Cdkl5*-null mouse models (Wang et al, 2012; Amendola et al., 2014) that recapitulate many core features of CDKL5 disorder and will constitute a fundamental support for future studies of the pathology.

Given the huge repercussion of *CDKL5* mutations on the central nervous system, the majority of studies described in literature are focused on post-mitotic neuronal cells; however, very recently it has been demonstrated that CDKL5 also has a role in proliferating cells (Valli et al., 2012; Fuchs et al., 2014). In fact, it has been shown that neuronal progenitor cells (NPCs) from *Cdkl5*-null mice present a higher proliferative index in comparison with control cells; this aberrant proliferation is immediately followed by increased apoptosis and a reduced capacity of new-born neurons to differentiate into mature neurons (Fuchs et al., 2014).

Considering all the above, we decided to investigate the role of CDKL5 in proliferating cells, paying particular attention on mitosis. Mitosis is divided into five phases: *prophase*, characterized by chromosome condensation and by the movement of centrosomes to the opposite poles of the cell; *prometaphase*, in which the nuclear membrane fully dissolves and the mitotic spindles capture and congress chromosomes to the equator of the cell (metaphase plate); *metaphase*, characterized by the complete alignment of chromosomes on the metaphase plate; *anaphase*, in which sister chromatids separate and migrate to opposite poles of the cell and *telophase*, in which the nuclear membrane reassembles, chromosomes decondense, and cytokinesis produces two equivalent daughter cells (O'Connor, 2008). Live-cell microscopy permitted us to demonstrate that the ablation of CDKL5 in HeLa cells causes an increase of the time spent in prometaphase and in telophase; this result is consistent with the increased mitotic index that we observed in silenced cells. Prolonged mitosis is often caused by a delay in satisfying the spindle assembly checkpoint due to improper centrosome functions that impede spindle formation (Su et al., 2000). The link between the observed phenotype and centrosome defects appeared very attractive; in fact, we have recently published that MeCP2 accumulates at the centrosome and is able to affect spindle formation and/or cell plane division (Bergo et al., 2015). Considering the functional inter-talk between the two proteins, we found it relevant to characterize

the subcellular localization of CDKL5 during cell cycle; interestingly, we found that CDKL5 does indeed localize at the centrosome from prophase to anaphase where after it moves from the centrosome to the midbody structure. We consistently observed this phenomenon in several human and rodent cell lines.

The centrosome is a central component of the cytoskeletal structure and consists of a scaffold core containing a large number of proteins including γ-tubulin and the γ-tubulin complex (γ-TuRC) that typically surrounds a pair of cylindrical centrioles enclosed in the amorphous pericentriolar material (PCM) (Schatten, 2008). During interphase the centrosome is involved in organizing an astral array of microtubules that participate in fundamental cellular functions such as cell motility, cell adhesion, and cell polarity (Bettencourt-Dias et al., 2007; Nigg et al., 2009). In proliferating cells, centrosome duplication occurs during the S-phase of the cell cycle, and, by the time a cell enters mitosis, it contains two centrosomes, which participate in the assembly and organization of the mitotic spindle (Glotzer, 2009; Lim et al., 2009).

Numerous cell cycle regulatory molecules have been identified at the centrosomes, which are thought to function as integration sites for the regulation of cell division progression (Doxsey et al., 2005b). For example the serine/threonine checkpoint kinase 2 (CHK2) is a centrosomal protein required for proper assembly of mitotic spindles and for chromosomal stability. Its depletion causes mitotic spindle defects associated with prolonged mitosis (Stolz et al., 2010; Chouinard et al., 2013). Thus, we hypothesized the involvement of CDKL5 in the organization of the mitotic spindle and the midbody and addressed this question by analysing the organization of the two structures in cells interfered for *CDKL5.* Interestingly, we discovered that, even though the ablation of CDKL5 does not cause significant changes in the midbody structure (data not shown), it induces an increase of abnormal spindle assembly with 30% more multipolar spindles with respect to control cells. Moreover the down-regulation of the kinase induces an increase of chromosomal misalignment and micronuclei formation. Spindle geometry plays a critical role in the establishment of kinetochore–microtubule attachment (Gregan et al., 2011), so it is possible that the chromosomal misalignment and the presence of micronuclei observed in silenced cells could be the consequence of aberrant spindle assembly. Re-introduction of wild-type CDKL5 completely restored spindle

defects indicating the specific role of the kinase in spindle organization. Notably time-lapse microscopy did not show any effect in cell viability or division failure suggesting that cells are able to bypass the defects described above, segregating their chromosomes, albeit with reduced fidelity demonstrated by the increased formation of micronuclei. The fact that we did not observe any significant cytokinesis failure suggests that CDKL5 does not play a role in the strict organization of this structure. However, we speculate that the kinase might represent a signal for the further progression in the cell cycle and that its inactivation/depletion might constitute a temporary stop. It is relevant to remember that cyclin-dependent kinases (CDKs) are key regulators of cell cycle progression, and that one of the mechanisms used to ensure that division is not initiated until chromosomes have been separated, is a block of cytokinesis through the inhibition of CDKs activity (Guertin et al., 2002).

When we analysed neuronal cells, we found that CDKL5 localizes at the centrosome of primary hippocampal neurons (data not shown) and neuronal precursor cells (NPCs), where the centrosomal accumulation can be observed also in interphase suggesting a cell-specific mechanism of this localization. It is worth recalling that the importance of the centrosome is not limited only to proliferating cells. In fact, the centrosome is widely accepted to be crucial for proper brain development and mutations in genes encoding centrosomal proteins cause severe neurodevelopmental disorders, such as lissencephaly (*LIS1*), microcephaly (*ASPM, MCPH1*), schizophrenia (*PCM1*) (Kuijpers & Hoogenraad, 2011), juvenile myoclonic epilepsy (*EFHC1*) (De Nijs et al., 2012) and, of relevance, classic Rett syndrome (*MECP2*) (Bergo et al., 2015). In the latter case, as mentioned before, even if mutations in *CDKL5* and *MECP2* give rise at two distinct diseases, molecular evidence suggest that they belong to a common molecular pathway that could explain the partial phenotypic overlap between classic RTT and CDKL5 disorder. The fact the both proteins localize at the centrosome in proliferating and non-proliferating cells could offer new interesting insights for the studies of these pathologies. In particular, given that MeCP2 is a substrate of CDKL5 (Mari et al., 2005), it will be interesting in the future to understand the nature of this common localization, investigating, in particular, if the presence of MeCP2 at the centrosome is mediated by a CDKL5-dependent phosphorylation event.

In conclusion, with this study we demonstrated that CDKL5 is a centrosomal protein implicated in the regulation of spindle assembly and in mitosis progression. It is plausible that previous defects associated with dysfunctional CDKL5 such as the impaired neuronal migration (Chen et al., 2010) and the aberrant proliferation/differentiation of neuronal progenitor cells (Fuchs et al., 2014), as well as the phenotypic outcome observed in CDKL5 disorder, might in part depend on the alteration of centrosomal functions. Future studies will focus on the analysis of cell cycle division and spindle assembly in *Cdkl5*$^{-/-}$ neuronal progenitors.

3.2 CDKL5 influences microtubules dynamics and is necessary for a stable IQGAP1-RAC1-CLIP170 complex formation

The centrosome is the main site of microtubule nucleation in most cells, so it is not surprising that many centrosomal proteins also take part in the organization of microtubules (Doxey, 2001; Tamura et al., 2012). Thus, we decided to investigate the role of CDKL5 in cytoskeleton dynamics and observed that its ablation induces a complete disorganization of the microtubule cytoskeleton. This was particularly evident when microtubule nucleation was stimulated with drug-induced depolymerisation. In fact, CDKL5 depletion causes a marked change in the re-configuration of astral microtubules highlighted by the loss of the radial array typical of COS7 cells. Despite this, no difference in the ability of microtubules to polymerize was observed, thus, since CDKL5 not localizes with centrosome during interphase, the aberrant cytoskeleton phenotype that we observed after its ablation probably is not due to impaired assembly/disassembly of polarized cytoskeletal polymers but rather to their defective interaction with binding proteins and molecular motors responsible for their movement and/or assembly into higher order structures.

In a yeast two-hybrid screening we identified IQGAP1 as a novel interactor of CDKL5. IQGAP1 is a 190 kDa scaffold protein that facilitates the formation of complexes implicated in the regulation of cytoskeletal dynamics, intracellular signalling and interactions (Hedman et al., 2015). One peculiarity of IQGAP1 is its

ability to act as a bridge between actin and microtubules. Through its CH domain, IQGAP1 directly recruits and supports actin polymerization (Mateer et al., 2004; Le et al., 2007; Watanabe et al., 2004), whereas the GRD and RGCT domains serve to recruit respectively Rho GTPases, as Rac1 and Cdc42, (Jacquemeta et al., 2014), and many TIPs as APC (Tirnauer, 2004), CLIP170 (Fukata et al., 2002), Clasp2 (Watanabe et al., 2009), and EB1 (Zhang et al., 2009). Contrary to the GAP proteins that induce GTP hydrolysis through the GRD domain, IQGAP1 preferentially binds and maintains the active form (GTP-bound) of Cdc42 and Rac1 by inhibiting the intrinsic GTPase activity (Hart et al., 1996; Kuroda et al., 1996; Kurella et al., 2009). IQGAP1 interacts with actin filaments and cross-links them in the presence of activated Rac1 and Cdc42 (Brandt et al., 2007; Le Clainche et al., 2007); the depletion of IQGAP1 prevents the formation of the actin meshwork at the leading edge and slows down cell migration (Watanabe et al., 2004). In the present study, we show that CDKL5 and IQGAP1 co-localize at the leading edge of migrating cells and that the depletion of CDKL5 impedes the localization of IQGAP1 at the cell cortex. Moreover, consistently with data described in literature (Chen et al., 2010), we demonstrated that the ablation of CDKL5 impairs cells migration. Further studies will be necessary to clarify if the aberrant localization of IQGAP1 at the leading edge is a direct consequence of the missing interaction with CDKL5, or if it is indirectly caused by a global effect of CDKL5 ablation on actin polymerization. In any case, the presence of IQGAP1 at the leading edge is fundamental not only for actin organization but also for microtubule stabilization. Indeed, it has been demonstrated that activated Rac1 binds IQGAP1 favouring the association of the scaffold protein with CLIP170 and permitting the stabilization of microtubules at the cell periphery (Fukata et al., 2002); in this regard, we demonstrated that the ablation of CDKL5 reduces the ability of IQGAP1 to interact with both Rac1 and CLIP170, suggesting that CDKL5 might be necessary for the stabilization of the plus ends of microtubules. Interestingly, IQGAP1 and CLIP170 cooperate to establish proper dendritic neuronal morphology. Indeed, the knockdown of these two proteins simplifies dendritic arborisation (Swiech et al., 2011), a phenotype that is also caused by the absence of CDKL5 (Chen et al., 2010, Amendola et al., 2014).

Whether CDKL5 phosphorylates IQGAP1 and the functional role of such an event still remain to be established. *In vitro* studies have indicated that the phosphorylation of IQGAP1 in Ser1441 and Ser1443 by PKC induces a conformational change releasing IQGAP1 from its autoinhibitory structure facilitating its interaction with Cdc42 (Grohmanova et al., 2004). Therefore, we envisage that CDKL5, by phosphorylating IQGAP1, might induce a conformational change that promotes the binding of Rac1 and subsequently CLIP170, thus favouring microtubule organization and dendrite arborisation.

In such a scenario a correct cooperation among the CDKL5-IQGAP1-Rac1-CLIP170 proteins would be fundamental to build a precise microtubule network: in particular, it seems that CDKL5 occupies a central role in the regulation of the interaction between IQGAP1 and its effector proteins Rac1 and CLIP170. However, whether CDKL5 acts as an effector or a regulator of Rac1 still remains an open question. It has been demonstrated that the activation of Rac1 is necessary to bring CDKL5 and IQGAP1 to the cell cortex (Fukata et al. 2002; Chen et al., 2010). Thus, one possible hypothesis is that activated Rac1 may determine specific sites close to the plasma membrane allowing the recruitment of CDKL5 and IQGAP1.

As a consequence the interaction with CDKL5 would induce a conformational change in IQGAP1 enhancing its interaction with Rac1 and thus favouring microtubule stabilization on the cell cortex via CLIP170.

3.3 Conclusions

In conclusion, we speculate that CDKL5 is an important regulator of cytoskeleton dynamics acting both during cell division and in quiescent cells. Indeed, during mitosis, it localizes at the centrosome regulating spindle organization and favouring correct chromosome alignment. In telophase it moves to the midbody probably supporting cytokinesis progression. In interphase, in response to proper stimuli (i.e. cellular polarization), it accumulates at the cellular cortex, where it regulates microtubule organization through specific effector proteins (Fig.21).

In the light of these findings, we provide a new mechanism that could explain how CDKL5 impacts neuronal morphology in CDKL5 disorder, opening new prospective for the implementation of future therapeutic strategies.

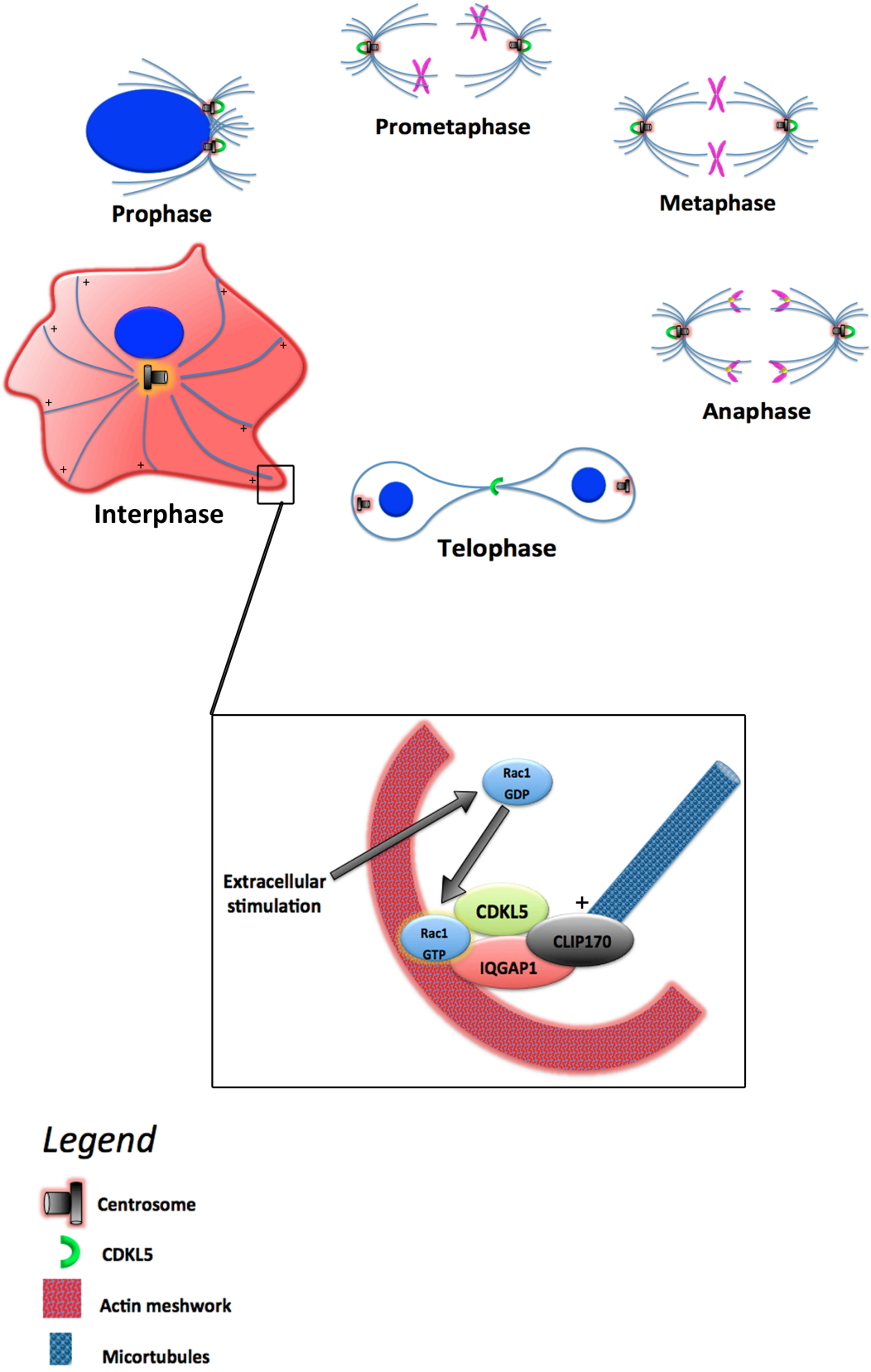

Figure 21 Proposed working model of CDKL5 functions in mitotic phases and at the cell cortex. From prophase to anaphase CDKL5 localizes at the centrosome regulating spindle organization and favouring correct chromosome alignment. In telophase it moves to the midbody probably supporting cytokinesis

progression. In interphase extracellular signal activate Rac1 and GEFs proteins at leading edges. Activated Rac1 marks spots where CDKL5 and IQGAP1 are recruited. There CDKL5 interacts/phosphorylates IQGAP1 and enhances the IQGAP1-Rac1 interaction favouring microtubule stabilization on the cell cortex through CLIP170.

4. MATERIALS AND METHODS

4.1 Plasmids

GFP-CDKL5, expressing the 107 kDa hCDKL5 isoform has been described elsewhere (Williamson 2012). pCAGGS-CDKL5-ires-GFP was cloned by inserting an EcoRI-EcoRV digested PCR product containing the murine CDKL5 cDNA (NP_0010795) into pCAGGS-ires-GFP digested with EcoRI and SmaI. pEGFP-IQGAP1 (plasmid 30112 deposited by David Sacks, Ren et al., 2005).

4.2 Antibodies

The following antibodies (Abs) were used: anti-γ-tubulin (Sigma-Aldrich, T5326), anti-α-tubulin (Sigma-Aldrich, T6074), anti-CDKL5 (Sigma-Aldrich, HPA002847), anti-GFP (Roche, 1814460), anti-PLK-1 (Santa Cruz, sc-17783; 1:200 dilution), anti-IQGAP1 (Santa Cruz, sc-10792), anti Rac1 (BD Transduction Laboratories, 610650), anti-CLIP170 (Genetex, GTX117504), Phalloidin-TRITC Conjugates (Sigma-Aldrich), anti-histone H3-Ser(P)-10 (Abcam, catalog no. ab1791). HRP-conjugated goat anti-mouse or anti-rabbit secondary Abs for immunoblotting were purchased from Thermo Scientific. DAPI and secondary Alexa Fluor anti-rabbit and anti-mouse Abs for immunofluorescence were obtained from Life Technologies Corporation.

4.3 Cell cultures, transfections and RNA interference (RNAi)

HeLa, MRC-5 and COS7 cells were maintained in DMEM (Dulbecco's modified Eagle's medium; Sigma-Aldrich) supplemented with 10% FBS, L-glutamine, 100 units/ml penicillin, and 100 μg/ml streptomycin at 37°C with 5% CO_2. Neuro-2A cells were maintained in MEM (Modified Eagle's medium; Sigma-Aldrich) supplemented with 10% FBS, L-glutamine, 100 units/ml penicillin, and 100 μg/ml streptomycin, 1% non essential aminoacids at 37°C with 5% CO_2. PC12 cells were

maintained in RPMI (Roswell Park Memorial Institute, Gibco) supplemented with 10% FBS, L-glutamine, 100 units/ml penicillin, and 100 μg/ml streptomycin at 37°C with 5% CO_2, for experiments these cells were seeded on poly-D-lysine coated coverslips.

For transfection, cells were cultured in 6- or 12-well dishes and transfected with plasmids using Lipofectamine™ 2000 (Life Technologies Incorporated) following the manufacturer's protocol. Cells were collected or fixed 24 h post-transfection. For siRNA transfection, 20 nM siRNA oligonucleotides targeting CDKL5 or a control siRNA (siCdkl5#1 5'CTATGGAGTTGTACTTAAA3', siCdkl5#2 5'GCAGAGTCGGCACAGCTAT3', siCtr. 5'CGUACGCGGAAUACUUCGATT3', siIqgap1 5'UGCCAUGGAUGAGAUUGGAUU3') were transfected into HeLa or MRC-5 cells using Lipofectamine™ RNAiMAX (Life Technologies Incorporated). For rescue experiments, a siRNA resistant pCAGGS-CDKL5-ires-GFP vector was transfected 60 h after CDKL5 silencing and cells analysed after another 24 h.

4.4 Western blotting (WB) and immunoprecipitation (IP)

Cells were lysed with lysis buffer (50 mM Tris-HCl pH 7.5, 150 mM NaCl, 1% Triton X-100, 1 mM EDTA) with addition of protease inhibitor cocktail (Sigma Aldrich) and PhosSTOP (Roche). After 30 min on ice, the lysates were clarified by centrifugation and the supernatants collected. Samples were separated by either 10% or 8% SDS-PAGE, transferred to nitrocellulose membranes, and blocked in 5% non-fat milk in TBS (20 mM Tris-HCl, pH 7.5, 150 mM NaCl) with 0.2% Tween-20 (T-TBS). Blots were incubated with primary Abs overnight at 4°C, washed in T-TBS, and incubated with appropriate secondary Abs for 1 h at room temperature. After extensive washes, blots were developed with either West PICO Chemiluminescence kit (Pierce) or with ECL Prime Western Blotting Detection Reagent (GE Healthcare Life Sciences).

For immunoprecipitation experiments, 1 mg of a mouse brain extract (post-natal day 9, P9) or HeLa cells were lysed in lysis buffer (50 mM Tris-HCl pH 7.5, 150 mM NaCl, 1% Triton X-100, 1 mM EDTA, 1 mM EGTA) with addition of protease inhibitor cocktail (Sigma Aldrich) and PhosSTOP (Roche) and incubated overnight at 4°C with 1 μg of anti-CDKL5, anti-IQGAP1, anti-CLIP170 or unrelated IgGs as

control. The immunocomplexes were precipitated with protein-G Agarose (Life Technologies) or with EZview™ Red Anti-c-Myc Affinity Gel (Sigma Aldrich), washed with lysis buffer and analysed by SDS-PAGE.

4.5 Immunofluorescence (IF)

For the staining of γ-tubulin and centrosome associated proteins, cells were permeabilized before fixation in PHEM (60 mM Pipes, 25 mM Hepes, 10 mM EGTA, and 2 mM $MgCl_2$) with 0.5% Triton X-100 for 2 min and then fixed in 4% paraformaldehyde. For all the other antibodies, cells were washed twice in PBS and fixed in 4% paraformaldehyde. For immunostaining, blocking solution (PBS, 5% horse serum, and 0.2% Triton X-100) was added for 1 h at room temperature before incubation with the appropriate primary antibodies overnight at 4°C. Slides were incubated with the designated secondary antibodies for 1 h at room temperature and washed with TBS. DNA was stained with DAPI (Life Technologies Incorporated), and slides were mounted with ProLong Gold antifade reagent (Life Technologies Incorporated). The analysis was performed with a NikonEclipse Ni upright microscope.

4.6 Centrosomal fractionation

Centrosome fractionation was performed as previously described (Bergo et al., 2015). Briefly, exponentially growing cells were treated with 10 μg/ml nocodazole and 5 μg/ml Cytochalasin B (both from Sigma-Aldrich) for 3 h, followed by hypotonic lysis. Centrosomes were harvested by centrifugation onto a 20% ficoll cushion and further purified by centrifugation through a discontinuous (70%, 50% and 40%) sucrose gradient. Fractions of 0.3 ml were collected and analysed by WB.

4.7 Neurosphere preparation

Neurospheres were prepared as previously described (Bedogni et al., 2015). Briefly, E15.5 embryos were individually dissected in PBS and the neocortex was transferred in Dulbecco's Modified Eagle Medium/F12 (DMEM) and dissociated by

extensive enzymatic digestion with Papaine (Sigma). Cells were then grown in medium containing DMEM/F12, 0.66% glucose, L-glutamine 1%, Pen/Strep 1%, 4 μg/mL of heparin, hormone mix with the addition of either 20 ng/mL epidermal growth factor (EGF) and 10 ng/mL basic fibroblast growth factor (bFGF) or bFGF alone. In such conditions, cells spontaneously formed neurospheres. Neurospheres were then dissociated in single-cell cultures and plated on matrigel-coated coverslips (BD Bioscience). IF was performed as described above.

4.8 Live-cell imaging

Cells were seeded in slides 8-well (80826, ibiTreat, Ibidi) and observed under an Eclipse Ti inverted microscope (Nikon) using a 40x objective. During the observation, cells were kept in a microscope stage incubator at 37°C and 5% CO_2. DIC images were acquired over a 24 h period by using a DS-Qi1Mc camera. Image and video processing were performed with NIS-Elements AR 3.22.

4.9 Microtubule Nucleation Assay

Microtubules were disrupted by incubating COS7 cells with 10 μg/ml nocodazole for 3 h. To assess microtubule regrowth, cells were washed twice with warm media to remove nocodazole and then incubated at 37 °C for different times. Fixed cells were stained with anti α-tubulin antibody and analysed for nucleation capacity and aster size. For determining aster size, images were taken from independent experiments, and each aster was treated independently. Quantification of the aster area was obtained using ImageJ software by drawing a region of interest around the aster and measuring the area of this region.

4.10 Wound healing assay

COS7 cells (10000 cells/well MW24) were transfected with the indicated siRNAs. After three days, confluent cells were scratched with a 200 μl tip and allowed to polarize and migrate for 5 h.

5. SUPPLEMENTAL MATERIAL

Movie 1 and 2 respectively show time lapse microscopy of HeLa cell interfered with control and Cdkl5#1 siRNAs.

6. ACKNOWLEDGEMENTS

Before starting it's better to seek advice from expert guides…

For this reason, it is my duty to say thank you to Prof. Charlotte Kisltrup-Nielsen for guiding me in this wonderful way, leaving me free to grow without hindering my ideas, criticizing my hypothesis where necessary and giving me credit when they were right.
Thanks to Prof. Nicoletta Landsberger for giving me the opportunity to take part of this world and to have contributed to my scientific growth offering me always precious advice.

To go on, it could be necessary to engage valuable collaborators...

Thanks to Prof. Silva Soddu and Dr. Cinzia Rinaldo for live cell imaging experiments performed at Nikon Reference Centre, CNR Institute of Molecular Biology and Pathology.
Thanks to Chetan Chandola for having contributed to this thesis.

To grow up you need to get in touch with the experience...

For this an infinite thanks to Laura Rusconi and Anna Bergo, to which I bring all my respect as very valid researchers, patients wives and caring mothers. A thousand thanks for all the time that you guided and supported me, for your teachings and for the sincere affection that you have shown me.

To work well you have to fell good...

So thanks to Marta Strollo and Gilda Stefanelli to be whom they are, for the many words of comfort, for the light heartedness of our Friday, for the serenity that you have been able to give me. Many thanks to Marco Tramarin to be my "anti-stress", but above all thanks because, despite everything, I can always trust on you (and vice versa;)).
Thanks to my old colleagues Dalila Ciceri, Paolo La Montanara, Marilena Valente and Sarfaraz Nawaz for the wise advice and the much laughter.
Thanks to Barbara Leva, Maria Fazzari and Diana Peroni for the help that you give me.

To be objective you have to keep in touch with reality...

Thanks to my parents for the infinite love that surround me without asking anything in return. Thanks to my family for the strong support. Thanks to Chiara, Giulia, Eleanora, Sara, Martina and to all my friends for putting up with the sudden changes of my mood and to be always present.

Thanks to my eternal accomplice Pasquale for listening, understanding and counselling me, for all the strength that you give me, because you believe in me... thanks for being part of my life.

In small doses we slowly take consciousness of ourselves, thus everything is clear, the aspiration to understand what still has not been proven, is nothing but our primordial desire of knowledge that we can not ignore because it's part of us and makes us slaves of a destiny that we are immensely grateful to have received…

7. BIBLIOGRAPHY

Amendola E, Zhan Y, Mattucci C, Castroflorio E, Calcagno E, Fuchs C, Lonetti G, Silingardi D, Vyssotski AL, Farley D, Ciani E, Pizzorusso T, Giustetto M, Gross CT. (2014). Mapping pathological phenotypes in a mouse model of CDKL5 disorder. PLoS One. 9(5):e91613.

Armstrong DD. (2005) Neuropathology of Rett syndrome. J Child Neurol. 20:747-53.

Artuso R, Mencarelli MA, Polli R, Sartori S, Ariani F, Pollazzon M, Marozza A, Cilio MR, Specchio N, Vigevano F, Vecchi M, Boniver C, Dalla Bernardina B, Parmeggiani A, Buoni S, Hayek G, Mari F, Renieri A, Murgia A. (2010). Early-onset seizure variant of Rett syndrome: definition of the clinical diagnostic criteria. Brain Dev. 32:17-24.

Azimzadeh J, Bornens M. (2007). Structure and duplication of the centrosome. J Cell Sci. 120(Pt 13):2139-42.

Bahi-Buisson N, Nectoux J, Rosas-Vargas H, Milh M, Boddaert N, Girard B, Cances C, Ville D, Afenjar A, Rio M, Héron D, N'guyen Morel MA, Arzimanoglou A,Philippe C, Jonveaux P,Chelly J,Bienvenu T. (2008a). Key clinical features to identify girls with CDKL5 mutations. Brain. 131:2647-61.

Bahi-Buisson N, Kaminska A, Boddaert N, Rio M, Afenjar A, Gérard M, Giuliano F, Motte J,Héron D,Morel MA,Plouin P,Richelme C,des Portes V,Dulac O,Philippe C,Chiron C, Nabbout R, Bienvenu T. (2008b) The three stages of epilepsy in patients with CDKL5 mutations. Epilepsia. 49:1027-37.

Bedogni F, Cobolli Gigli C, Pozzi D, Rossi RL, Scaramuzza L, Rossetti G, Pagani M, Kilstrup-Nielsen C, Matteoli M, Landsberger N. (2015). Defects During Mecp2 Null

Embryonic Cortex Development Precede the Onset of Overt Neurological Symptoms. Cereb Cortex. pii: bhv078.

Bergo A, Strollo M, Gai M, Barbiero I, Stefanelli G, Sertic S, Cobolli Gigli C, Di Cunto F, Kilstrup-Nielsen C, Landsberger N. (2015). Methyl-CpG binding protein 2 (MeCP2) localizes at the centrosome and is required for proper mitotic spindle organization. J Biol Chem. 290(6):3223-37.

Bertani I, Rusconi L, Bolognese F, Forlani G, Conca B, De Monte L, Badaracco G, Landsberger N, Kilstrup-Nielsen C. (2006). Functional consequences of mutations in
CDKL5, an X-linked gene involved in infantile spasms and mental retardation. J Biol Chem. 281:32048-56.

Bettencourt-Dias M, Glover DM. (2007). Centrosome biogenesis and function: centrosomics brings new understanding. Nat Rev Mol Cell Biol. 8(6):451-63.

Bourdon V, Philippe C, Labrune O, Amsallem D, Arnould C, Jonveaux P. (2001). A detailed analysis of the MECP2 gene: prevalence of recurrent mutations and gross DNA rearrangements in Rett syndrome patients. Hum Genet. 108:43-50.

Brandt DT, Grosse R. (2007). Get to grips: steering local actin dynamics with IQGAPs. EMBO Rep. 8(11):1019-23.

Carouge D, Host L, Aunis D, Zwiller J, Anglard P. (2010). CDKL5 is a brain MeCP2 target gene regulated by DNA methylation. Neurobiol Dis. 38:414-24.

Chahrour, M and Zoghbi, H. Y. (2007) The story of Rett syndrom from clinical to neurobiology. Neuron 56, 422-437

Cheadle JP, Gill H, Fleming N, Maynard J, Kerr A, Leonard H, Krawczak M, Cooper DN, Lynch S, Thomas N, Hughes H, Hulten M, Ravine D, Sampson JR, Clarke A. (2000). Long- read sequence analysis of the MECP2 gene in Rett syndrome

patients: correlation of disease severity with mutation type and location. Hum Mol Genet. 12, 1119-1129.

Chen Q, Zhu YC, Yu J, Miao S, Zheng J, Xu L, Zhou Y, Li D, Zhang C, Tao J, Xiong ZQ. (2010). CDKL5, a protein associated with rett syndrome, regulates neuronal morphogenesis via Rac1 signaling. J Neurosci. 30:12777-86.

Chen J, Alberts I, Li X. (2014) Dysregulation of the IGF-I/PI3K/AKT/mTOR signaling pathway in autism spectrum disorders. Int J Dev Neurosci. 35:35-41.

Chouinard G, Clément I, Lafontaine J, Rodier F, Schmitt E. (2013). Cell cycle-dependent localization of CHK2 at centrosomes during mitosis. Cell Div. 8(1):7

Williamson SL, Christodoulou J. (2006). Rett syndrome: new clinical and molecular insights. Eur J Hum Genet. 14(8):896-903.

Cobbold C, Coventry J, Ponnambalam S, Monaco AP. (2003). The Menkes disease ATPase (ATP7A) is internalized via a Rac1-regulated, clathrin- and caveolae-independent pathway. Hum Mol Genet. 12(13):1523-33.

De Nijs L, Wolkoff N, Coumans B, Delgado-Escueta AV, Grisar T, Lakaye B. (2012). Mutations of EFHC1, linked to juvenile myoclonic epilepsy, disrupt radial and tangential migrations during brain development. Hum Mol Genet. 21(23):5106-17.

Doxsey S. (2001). Re-evaluating centrosome function. Nat Rev Mol Cell Biol. 2(9):688-98.

Doxsey S, McCollum D, Theurkauf W. (2005). Centrosomes in cellular regulation. Annu Rev Cell Dev Biol. 21:411-34.

Doxsey S, Zimmerman W, Mikule K. (2005b) Centrosome control of the cell cycle. Trends Cell Biol. 15(6):303-11.

Elia M, Falco M, Ferri R, Spalletta A, Bottitta M, Calabrese G, Carotenuto M, Musumeci SA, Lo Giudice M, Fichera M. (2008). CDKL5 mutations in boys with severe encephalopathy and early-onset intractable epilepsy. Neurology. 71:997-9.

Fehr S, Wilson M, Downs J, Williams S, Murgia A, Sartori S, Vecchi M, Ho G, Polli R, Psoni S, Bao X, de Klerk N, Leonard H, Christodoulou J. (2013). The CDKL5 disorder is an independent clinical entity associated with early-onset encephalopathy. Eur J Hum Genet. 21(3):266-73.

Fehr S, Leonard H, Ho G, Williams S, de Klerk N, Forbes D, Christodoulou J, Downs J. (2015). There is variability in the attainment of developmental milestones in the CDKL5 disorder. J Neurodev Disord. 7(1):2.

Fuchs C, Trazzi S, Torricella R, Viggiano R, De Franceschi M, Amendola E, Gross C, Calzà L, Bartesaghi R, Ciani E. (2014). Loss of CDKL5 impairs survival and dendritic growth of newborn neurons by altering AKT/GSK-3β signaling. Neurobiol Dis. 70:53-68

Fukata M, Nakagawa M, Itoh N, Kawajiri A, Yamaga M, Kuroda S, Kaibuchi K. (2001). Involvement of IQGAP1, an effector of Rac1 and Cdc42 GTPases, in cell-cell dissociation during cell scattering. Mol Cell Biol. 21(6):2165-83.

Fukata M, Watanabe T, Noritake J, Nakagawa M, Yamaga M, Kuroda S, Matsuura Y, Iwamatsu A, Perez F, Kaibuchi K. (2002). Rac1 and Cdc42 capture microtubules through IQGAP1 and CLIP-170. Cell. 109(7):873-85.

Gage FH. (2000). Mammalian neural stem cells. Science. 287:1433–1438.

Glotzer M. (2009). The 3Ms of central spindle assembly: microtubules, motors and MAPs. Nat Rev Mol Cell Biol. 10(1):9-20.

Gregan J, Polakova S, Zhang L, Tolić-Nørrelykke IM, Cimini D. (2011). Merotelic kinetochore attachment: causes and effects. Trends Cell Biol. 21(6): 374–381.

Grohmanova K, Schlaepfer D, Hess D, Gutierrez P, Beck M, Kroschewski R. (2004). Phosphorylation of IQGAP1 modulates its binding to Cdc42, revealing a new type of rho-GTPase regulator. J Biol Chem. 279(47):48495-504.

Guertin DA, Trautmann S, McCollum D. (2002). Cytokinesis in eukaryotes. Microbiol Mol Biol Rev. 66(2):155-78.

Hagberg BA, Skjeldal OH. (1994). Rett variants: a suggested model for inclusion criteria. Pediatr Neurol. 11:5–11.

Hagberg B. (2005). Rett syndrome: long-term clinical follow-up experiences over four decades. J Child Neurol. 20(9):722-7.

Hagne I, Witt-Engerström I, Hagberg B. (1989). EEG development in Rett syndrome. A study of 30 cases. Electroencephalogr Clin Neurophysiol. 72(1):1-6.

Hanefeld F. (1985). The clinical pattern of the Rett syndrome. Brain Dev. 7:320–325.

Hart MJ1, Callow MG, Souza B, Polakis P. (1996). IQGAP1, a calmodulin-binding protein with a rasGAP-related domain, is a potential effector for cdc42Hs. EMBO J. 15(12):2997-3005.

Hayashi MT, Karlseder J. (2013). DNA damage associated with mitosis and cytokinesis failure. Oncogene. 32(39):4593-601

Hedman AC, Smith JM, Sacks DB. (2015). The biology of IQGAP proteins: beyond the cytoskeleton. EMBO Rep. 16(4):427-46.

Hu CK, Coughlin M, Mitchison TJ. (2012). Midbody assembly and its regulation during cytokinesis. Mol Biol Cell. 23(6):1024-34.

Huopaniemi L, Tyynismaa H, Rantala A, Rosenberg T, Alitalo T (2000). Characterisation of two unusualRS1gene deletions segregating in Danish retinoschisis families. Hum Mutat 16:307-314.

Brown CJ. (1999). Skewed X-chromosome inactivation: cause or consequence? J Natl Cancer Inst. 91(4):304-5.

Jacquemet G, Humphries MJ. (2013). IQGAP1 is a key node within the small GTPase network. Small GTPases. 4(4):199-207.

Kalscheuer VM, Tao J, Donnelly A, Hollway G, Schwinger E, Kübart S, Menzel C,Hoeltzenbein M,Tommerup N,Eyre H,Harbord M,Haan E,Sutherland GR,Ropers HH, Gécz J. (2003). Disruption of the serine/threonine kinase 9 gene causes severe X- linked infantile spasms and mental retardation. Am J Hum Genet. 72:1401-11.

Kameshita I, Sekiguchi M, Hamasaki D, Sugiyama Y, Hatano N, Suetake I, Tajima S, Sueyoshi N. (2008). Cyclin-dependent kinase-like 5 binds and phosphorylates DNA methyltransferase 1. Biochem Biophys Res Commun. 377:1162-7.

Katayama S, Sueyoshi N, Kameshita I. (2015). Critical Determinants of Substrate Recognition by Cyclin-Dependent Kinase-like 5 (CDKL5). Biochemistry. 54(19):2975-87.

Kilstrup-Nielsen C, Rusconi L, La Montanara P, Ciceri D, Bergo A, Bedogni F, Landsberger N (2012). What we know and would like to know about CDKL5 and its involvement in epileptic encephalopathy. Neural Plast. 2012:728267.

Krause M, Gautreau A. (2014). Steering cell migration: lamellipodium dynamics and the regulation of directional persistence. Nat Rev Mol Cell Biol. 15(9):577-90.

Kuijpers M, Hoogenraad CC. (2011) Centrosomes, microtubules and neuronal development. Mol Cell Neurosci.48(4):349-58.

Kurella VB1, Richard JM, Parke CL, Lecour LF Jr, Bellamy HD, Worthylake DK. (2009) Crystal structure of the GTPase-activating protein-related domain from IQGAP1. J Biol Chem. 284(22):14857-65.

Kuroda S, Fukata M, Kobayashi K, Nakafuku M, Nomura N, Iwamatsu A, Kaibuchi K. (1996). Identification of IQGAP as a putative target for the small GTPases, Cdc42 and Rac1. J Biol Chem. 271(38):23363-7.

La Montanara P, Rusconi L, Locarno A, Forti L, Barbiero I, Tramarin M, Chandola C, Kilstrup-Nielsen C, Landsberger N (2015). Synaptic synthesis, dephosphorylation, and degradation: a novel paradigm for an activity-dependent neuronal control of CDKL5. J Biol Chem. 290: 4512-4527.

Le Clainche C, Schlaepfer D, Ferrari A, Klingauf M, Grohmanova K, Veligodskiy A, Didry D, Le D, Egile C, Carlier MF, Kroschewski R. (2007). IQGAP1 stimulates actin assembly through the N-WASP-Arp2/3 pathway. J Biol Chem. 282(1):426-35. Cambiare in discu

Lim, H.H., Zhang, T., Surana, U. (2009). Regulation of centrosome separation in yeast and vertebrates: common threads. Trends Cell Biol. 19:325–333.

Malarkannan S, Awasthi A, Rajasekaran K, Kumar P, Schuldt KM, Bartoszek A, Manoharan N, Goldner NK, Umhoefer CM, Thakar MS. (2012). IQGAP1: a regulator of intracellular spacetime relativity. J Immunol. 188(5):2057-63.

Mari F, Azimonti S, Bertani I, Bolognese F, Colombo E, Caselli R, Scala E, Longo I, Grosso S, Pescucci C, Ariani F, Hayek G, Balestri P, Bergo A, Badaracco G, Zappella M, Broccoli V, Renieri A, Kilstrup-Nielsen C, Landsberger N. (2005). CDKL5 belongs to the same molecular pathway of MeCP2 and it is responsible for the early-onset seizure variant of Rett syndrome. Hum Mol Genet. 14:1935-46.

Mateer, S.C., Morris, L.E., Cromer, D.A., Bensenor, L.B., Bloom, G.S., (2004). Actin filament binding by a monomeric IQGAP1 fragment with a single calponin homology domain. Cell Motil. Cytoskeleton 58, 231–241.

Montini E, Andolfi G, Caruso A, Buchner G, Walpole SM, Mariani M, Consalez G, Trump D, Ballabio A, Franco B. (1998). Identification and characterization of a novel serine- threonine kinase gene from the Xp22 region. Genomics. 51:427-33.

Murakami N, Xie W, Lu RC, Chen-Hwang MC, Wieraszko A, Hwang YW. (2006). Phosphorylation of amphiphysin I by minibrain kinase/dual-specificity tyrosine phosphorylation-regulated kinase, a kinase implicated in Down syndrome. J Biol Chem. 281(33):23712-24.

Neul JL, Kaufmann WE, Glaze DG, Christodoulou J, Clarke AJ, Bahi-Buisson N, Leonard H, Bailey ME, Schanen NC, Zappella M, Renieri A, Huppke P, Percy AK; RettSearch Consortium (2010). Rett syndrome: revised diagnostic criteria and nomenclature. Ann Neurol. 68(6):944-50.

Nigg EA1, Raff JW. (2009).Centrioles, centrosomes, and cilia in health and disease. Cell. 139(4):663-78.

Nomura, Y. (2005). Early behavior characteristics and sleep disturbance in Rett syndrome. Brain Dev. 27 (Suppl 1), S35–S42.

O'Connor, C. Cell Division: Stages of Mitosis (2008). Nature Education 1(1):188

Ramakers GJ1. (2002). Rho proteins, mental retardation and the cellular basis of cognition. Trends Neurosci. 25(4):191-9.

Rett, A. (1966). On a unusual brain atrophy syndrome in hyperammonemia in childhood. Wien Med Wochenschr. 116(37):723-6.

Ricciardi S, Kilstrup-Nielsen C, Bienvenu T, Jacquette A, Landsberger N, Broccoli V (2009). CDKL5 influences RNA splicing activity by its association to the nuclear speckle molecular machinery. Hum Mol Genet. 18: 4590-4602.

Ricciardi S, Boggio EM, Grosso S, Lonetti G, Forlani G, Stefanelli G, Calcagno E, Morello N, Landsberger N, Biffo S, Pizzorusso T, Giustetto M, Broccoli V (2011). Reduced AKT/mTOR signaling and protein synthesis dysregulation in a Rett syndrome animal model. Hum Mol Genet. 20: 1182-1196.

Ricciardi S, Ungaro F, Hambrock M, Rademacher N, Stefanelli G, Brambilla D, Sessa A, Magagnotti C, Bachi A, Giarda E, Verpelli C, Kilstrup-Nielsen C, Sala C, Kalscheuer VM, Broccoli V (2012). CDKL5 ensures excitatory synapse stability by reinforcing NGL-1-PSD95 interaction in the postsynaptic compartment and is impaired in patient iPSC-derived neurons. Nat Cell Biol. 14:911-923.

Rosas-Vargas H, Bahi-Buisson N, Philippe C, Nectoux J, Girard B, N'Guyen Morel MA, Gitiaux C, Lazaro L, Odent S, Jonveaux P, Chelly J, Bienvenu T. (2007). Impairment of CDKL5 nuclear localisation as a cause for severe infantile encephalopathy. J Med Genet. 45:172-8.

Roze, E., Cochen, V., Sangla, S., Bienvenu, T., Roubergue, A., Leu-Semenescu, S., and Vidaihet, M. (2007). Rett syndrome: An overlooked diagnosis in women with stereotypic hand movements, psychomotor retardation, Parkinsonism, and dystonia. Mov. Disord. 22, 387–389.

Rusconi L, Salvatoni L, Giudici L, Bertani I, Kilstrup-Nielsen C, Broccoli V, Landsberger N. (2008). CDKL5 expression is modulated during neuronal development and its subcellular distribution is tightly regulated by the C-terminal tail. J Biol Chem. 283:30101-11.

Scala E, Ariani F, Mari F, Caselli R, Pescucci C, Longo I, Meloni I, Giachino D, Bruttini M, Hayek G, Zappella M, Renieri A. (2005). CDKL5/STK9 is mutated in Rett syndrome variant with infantile spasms. J Med Genet. 42:103-7.

Schatten, H. (2008). The mammalian centrosome and its functional significance. Histochem. Cell Biol. 129, 667–686.

Schmeisser MJ1, Ey E, Wegener S, Bockmann J, Stempel AV, Kuebler A, Janssen AL, Udvardi PT, Shiban E, Spilker C, Balschun D, Skryabin BV, Dieck St, Smalla KH, Montag D, Leblond CS, Faure P, Torquet N, Le Sourd AM, Toro R, Grabrucker AM, Shoichet SA, Schmitz D, Kreutz MR, Bourgeron T, Gundelfinger ED, Boeckers TM. (2012) Autistic-like behaviours and hyperactivity in mice lacking ProSAP1/Shank2. Nature 486(7402):256–260.

Sekiguchi M, Katayama S, Hatano N, Shigeri Y, Sueyoshi N, Kameshita I. (2013). Identification of amphiphysin 1 as an endogenous substrate for CDKL5, a protein kinase associated with X-linked neurodevelopmental disorder. Arch Biochem Biophys. 535(2):257-67.

Stolz A, Ertych N, Kienitz A, Vogel C, Schneider V, Fritz B, Jacob R, Dittmar G, Weichert W, Petersen I, Bastians H. (2010). The CHK2-BRCA1 tumour suppressor pathway ensures chromosomal stability in human somatic cells. Nat Cell Biol. 12(5):492-9.

Swiech L, Blazejczyk M, Urbanska M, Pietruszka P, Dortland BR, Malik AR, Wulf PS, Hoogenraad CC, Jaworski J. (2011). CLIP-170 and IQGAP1 cooperatively regulate dendrite morphology. J Neurosci. 31(12):4555-68.

Szafranski P, Golla S, Jin W, Fang P, Hixson P, Matalon R, Kinney D, Bock HG, Craigen W, Smith JL, Bi W, Patel A, Wai Cheung S, Bacino CA, Stankiewicz P. (2015). Neurodevelopmental and neurobehavioral characteristics in males and females with CDKL5 duplications. Eur J Hum Genet. 23(7):915-21.

Tamura N, Draviam VM. (2012). Microtubule plus-ends within a mitotic cell are 'moving platforms' with anchoring, signalling and force-coupling roles. Open Biol. ;2(11):120132.

Tao J, Van Esch H, Hagedorn-Greiwe M, Hoffmann K, Moser B, Raynaud M, Sperner J, Fryns JP, Schwinger E, Gécz J, Ropers HH, Kalscheuer VM. (2004). Mutations in the X- linked cyclin-dependent kinase-like 5 (CDKL5/STK9) gene are associated with severe neurodevelopmental retardation. Am J Hum Genet. 75:1149-54.

Tirnauer JS. (2004). A new cytoskeletal connection for APC: linked to actin through IQGAP. Dev Cell. 7(6):778-80.

Valli E, Trazzi S, Fuchs C, Erriquez D, Bartesaghi R, Perini G, Ciani E. (2012). CDKL5, a novel MYCN-repressed gene, blocks cell cycle and promotes differentiation of neuronal cells. Biochim Biophys Acta. 1819(11-12):1173-85.

Su TT, Vidwans SJ. (2000). DNA defects target the centrosome. Nat Cell Biol. 2(2):E28-9.

Wang IT, Allen M, Goffin D, Zhu X, Fairless AH, Brodkin ES, Siegel SJ, Marsh ED, Blendy JA, Zhou Z. (2012). Loss of CDKL5 disrupts kinome profile and event-related potentials leading to autistic-like phenotypes in mice. Proc Natl Acad Sci U S A. 109(52):21516-21.

Watanabe T, Wang S, Noritake J, Sato K, Fukata M, Takefuji M, Nakagawa M, Izumi N, Akiyama T, Kaibuchi K. (2004). Interaction with IQGAP1 links APC to Rac1, Cdc42, and actin filaments during cell polarization and migration. Dev Cell. 7(6):871-83.

Watanabe T, Noritake J, Kaibuchi K. (2005). Roles of IQGAP1 in cell polarization and migration. Novartis Found Symp. 269:92-101;

Watanabe T, Noritake J, Kakeno M, Matsui T, Harada T, Wang S, Itoh N, Sato K, Matsuzawa K, Iwamatsu A, Galjart N, Kaibuchi K. (2009). Phosphorylation of CLASP2 by GSK-3beta regulates its interaction with IQGAP1, EB1 and microtubules. J Cell Sci. 122(Pt 16):2969-79.

Weaving LS, Christodoulou J, Williamson SL, Friend KL, McKenzie OL, Archer H, Evans J, Clarke A, Pelka GJ, Tam PP, Watson C, Lahooti H, Ellaway CJ, Bennetts B, Leonard H, Gécz J. (2004). Mutations of CDKL5 cause a severe neurodevelopmental disorder with infantile spasms and mental retardation. Am J Hum Genet. 75:1079-93.

Williamson SL, Giudici L, Kilstrup-Nielsen C, Gold W, Pelka GJ, Tam PP, Grimm A, Prodi D, Landsberger N, Christodoulou J. (2012). A novel transcript of cyclin-dependent kinase-like 5 (CDKL5) has an alternative C-terminus and is the predominant transcript in brain. Hum Genet. 131:187-200.

Wittmann T, Waterman-Storer CM. (2001). Cell motility: can Rho GTPases and microtubules point the way? J Cell Sci. 114(Pt 21):3795-803.

Yang Z, Loncarek J, Khodjakov A, Rieder CL. (2008). Extra centrosomes and/or chromosomes prolong mitosis in human cells. Nat Cell Biol. 10(6):748-51.

Zhang, T., Zaal, K.J., Sheridan, J., Mehta, A., Gundersen, G.G., Ralston, E., (2009). Micro- tubule plus-end binding protein EB1 is necessary for muscle cell differentiation, elongation and fusion. J. Cell Sci. 122:1401–1409.

Zhao C1, Teng EM, Summers RG Jr, Ming GL, Gage FH. (2006). Distinct morphological stages of dentate granule neuron maturation in the adult mouse hippocampus. J Neurosci. 4;26(1):3-11.

Zhu YC, Li D, Wang L, Lu B, Zheng J, Zhao SL, Zeng R, Xiong ZQ. (2013). Palmitoylation-dependent CDKL5-PSD-95 interaction regulates synaptic targeting of CDKL5 and dendritic spine development. Proc Natl Acad Sci U S A. 110(22):9118-23.